Computers and Concrete, *Vol. 34, No. 6 (2024) 659-704*
https://doi.org/10.12989/cac.2024.34.6.659

Minimizing the cost of structural design of RC corbels: A hybrid approach of optimizing pattern search technology and artificial intelligence

Rabi' M. Najem[1], Salim T. Yousif*[2], James H. Haido[3], Shaker Qaidi[3], Honar Issa[4] and Bashar A. Mahmood[5]

[1]Department of Civil Engineering, College of Engineering, University of Mosul, Mosul, Iraq
[2]College of Engineering, Nawroz University, Duhok, Kurdistan Region, Iraq
[3]College of Engineering, University of Duhok, Duhok, Kurdistan Region, Iraq
[4]The American University of Kurdistan, Duhok, Kurdistan Region, Iraq
[5]Ministry of Labour and Social Affairs, Iraq

(*Received January 22, 2023, Revised March 20, 2024, Accepted April 11, 2024*)

Abstract. In the recent years, modeling of concrete properties based on optimization and prioritization methods has been performed using machine learning techniques including genetic programming, artificial neural networks (ANN), an adaptive neuro-fuzzy inference system, and support vector machines. However, the application of ANN to the task of optimizing the design of reinforced concrete (RC) corbels has been limited in previous studies. In this endeavor, two empirical mathematical models of ANN are developed to calculate the optimal reinforcement ratio and effective depth of RC corbel. More than 1,500 corbel data have been processed utilizing pattern search optimization and used in this computational artificial neural solution. Five model parameters were adopted to formulate simple ANN mathematical models. Parametric analysis was performed to justify the independent parameters of ANN models. This procedure showed the accuracy of ANN models, despite changes in independent parameters. Thus, these variables are successfully integrated into the neural models. The stability and simplicity of the proposed mathematical models of ANN make them suitable for optimizing the design of RC corbels, as these formulas are applicable to predict the optimal reinforcement ratio and edge impact depth, considering the cost factor.

Keywords: artificial neural networks (ANN); cost analysis; optimization; pattern search technique; RC corbels; reinforcement ratio

1. Introduction

Over the last few years, efforts have been made to optimize the design of RC structures and their components based on minimizing the required quantity of concrete and steel reinforcement. Reinforced concrete corbels (RCC) are described as short cantilevers that protrude from columns or walls and have shear slenderness, which is often less than unity. They are typically employed to withstand forces acting at the joints of precast floors or beams. Corbels are primarily designed to withstand vertical loads and horizontal forces generated by beams, bridge piers, or bridge crane shrinkage, creep, and thermal impacts. It became a more prevalent component in the construction of buildings as the use of precast concrete expanded. Owing to their low shear slenderness ratios, such components are typically categorized as having a D-region, which exhibits significant disruption in the strain distribution across the cross-section, even during the elastic behavior phase. Shear, rather than the bending moment, controls the dominant behavior of the RC corbels. ACI 318-19 (2019) regulations require corbels to have a shear slenderness ratio of less than two. Such elements can be designed using the strut-and-tie method (Özkal and Uysal 2017, Abdul-Razzaq and Dawood 2020, Chetchotisak *et al.* 2022) or using the shear-friction strategy for those with a shear slenderness ratio of less than one. Numerous previous studies (Mattock *et al.* 1976, Yong *et al.* 1985, Fattuhi and Hughes 1989, Foster *et al.* 1996, Torres 1998, Campione *et al.* 2007, Lu and Lin 2009, Ozden and Atalay 2011, Al-Shaarbaf *et al.* 2015, Ivanova and Assih 2015, Lachowicz and Nagrodzka-Godycka 2016, Ridha *et al.* 2017, Al-Kamaki *et al.* 2018, Mohammad and Al-Shamaa 2018, Souza *et al.* 2019, Shakir 2020) have been performed to experimentally examine the performance of RC corbels considering different shear slenderness ratios and concrete strength grades. The design criteria for these structural elements were compliant with known RC design codes.

On the other hand, some prior works were devoted to investigating the analytical and numerical solutions to predict the behavior of RC corbels. Mattock *et al.* (1976) developed some modified shear-friction models for the behavior of RC corbels with shear slenderness ratios (a/d) less than unity, the recommended stirrup reinforcement was calculated based on the shear strength of the corbel-RC column interface. Yong *et al.* (1985) validated the ACI Code shear-friction and truss analogy (STM) procedure for

*Corresponding author, Professor
E-mail: salim.yousif@nawroz.edu.krd

ISSN: 1598-8198 (Print), 1598-818X (Online)

RC corbels with shear slenderness ratios of 0.39 and strengths ranging from 41.4 to 82.7 MPa. The expected failure modes for the corbel structure were investigated analytically by Torres (1998), who considered six failure mechanisms based on concrete crushing and cracking. Campione *et al.* (2005) developed an analytical model to comply with the equivalent truss analogy, considering steel reinforcement and hooked steel fibers in concrete shear structures such as corbels. This analytical model was modified in Reference Campione *et al.* (2007) to be suitable for high-strength concrete steel-fiber corbels, the effect of volume fraction and arrangement of the fibers on the corbel flexural strength was investigated. It was concluded that the presence of fibers and steel stirrups achieve the adequate strength capacity of the corbels. Campione (2009) proposed a strut-tie model to compute the flexural behavior of RC corbels containing steel fibers without secondary steel reinforcement. The validity of this model was proven via a comparison of the calculated outputs with the experimental results. de Lima Araújo *et al.* (2021) modified the analytical models (Campione *et al.* 2007, Campione 2009) for monolithic RC corbels, depending on computational modeling, to use appropriate two-step non-monolithic RC corbels incorporating steel fibers.

The numerical analysis of the shear control structures, such as RC corbels and deep beams, was considered extensively in prior studies based on finite element simulation. Nonlinear finite element analysis of RC corbels was performed by Prasad *et al.* (1993) using an elastoplastic constitutive material model. The crack pattern of concrete was predicted by smeared-fixed cracking formulation. The finite element results showed good matching with experimental records for the performance of the corbels. Gao and Zhang (2010) adopted a nonlinear finite element method to analyze the response of steel-fiber RC corbels to examine the effect of fiber content on their shear behavior. Numerical solution refers to an increase in the shear strength of the corbel with increasing in fiber content. A Quasi-static finite element simulation of the performance of short RC corbels, with and without shear bars, was implemented by Syroka *et al.* (2011). Continuum constitutive models were used to simulate the concrete behavior, taking into account an isotropic damaging effect and smeared crack formation. The behavior of the reinforcement was modeled by an elastoplastic behavior model. The impact of fracture energy, due to compressive stresses, on concrete strain localization was investigated carefully. Asnake (2016) conducted a parametric study to evaluate the behavior of RC corbels using finite element analysis in ANSYS. Corbel dimensions and reinforcement, concrete compressive strength, and loading conditions were the main parameters. The analysis results exhibit remarkable agreement with those found by a strut-tie model. Parol *et al.* (2018) studied the influence of horizontal loading on the strength of RC corbels utilizing strut-tie models. They concluded that the shear stirrups have a trivial effect on the resistance of the corbel to the horizontal-vertical loading system if the structural failure is controlled by concrete crushing. The applicability of the equilibrium strut-tie method in the loading capacity prediction of RC corbels was evaluated by Adrija *et al.* (2021) employing previous experimental data in the literature. This analytical method gives reliable outcomes in agreement with the nonlinear finite element solution of these corbels in terms of crack failure mode and loads at failure. In the case of numerical simulation, the performance of RC corbels was predicted among others by Prasad *et al.* (1993), Strauss *et al.* (2006), Manzoli *et al.* (2008), Syroka *et al.* (2011), Canha *et al.* (2014), Abdul-Razzak and Ali (2011), Abu-Obaida *et al.* (2020), and Adrija *et al.* (2021).

Rules-of-thumb essential for structural design, like the biggest concrete size required for an RC corbel and the maximum weight of its steel reinforcement, along with the structural cost of the construction, have not retained promptness with the development of modern computational techniques. These analytical tools do not take into account the construction cost, which consequently leads to inefficient and outdated outcomes. The optimization of the structural design makes it conceivable to reach the best outcome for a known structural system by fully satisfying the imposed design constraints. Previous studies covered common optimization approaches to optimize the design of structural members such as beams, columns, slabs, etc. (DeRousseau *et al.* 2018, Nikbakht *et al.* 2019, Huang *et al.* 2020, Chiniforush *et al.* 2021, İpek *et al.* 2021, Pierott *et al.* 2021).

Regarding optimized design and analysis of RC corbels, there are a few works deserving mention like those given in references (Bruggi 2009, Amir 2013), but none of these prior works emphasizes the optimum cost design of RC corbels as far as the materials such as steel reinforcement, concrete, and framework are concerned, using the genetic algorithm approach. Bruggi (2009) used minimum compliance optimization, depending on finite element analysis outcomes, to generate a truss-and-tie-like design of 3D corbel models. This allows one to deal with design issues such as torsional steel bars and discontinuity zones in box-form RC structures. A published paper given by Amir (2013) proposed a new procedure utilizing topology optimization analysis to predict the structural load-bearing capacity per unit weight of concrete. Optimized outputs were compared with those of concrete design standards, it was demonstrated that the analysis procedure has a remarkable efficiency in generating efficacious RC corbels.

Smarslik *et al.* (2019) introduced a novel method of generating topology optimization with a contemplated bias toward compression or tension for applications in structural analysis. Assumptions were adopted in this optimizing procedure via a linear-elastic isotropic concrete material model and a combined truss and continuum topology with an orthotropic material model. The authors deduced that the biased solution is validated in the practical design of RC corbels based on assessments of their structural behavior, overall stability, and robustness. Mozaffari *et al.* (2020) bridged the gap between geometry-based analysis and numerical layout optimization to design RC structures complying with a strut-and-tie approach. A numerical technique for the simulation of the stress flow in the corbel structure was provided by Almeida *et al.* (2013). This

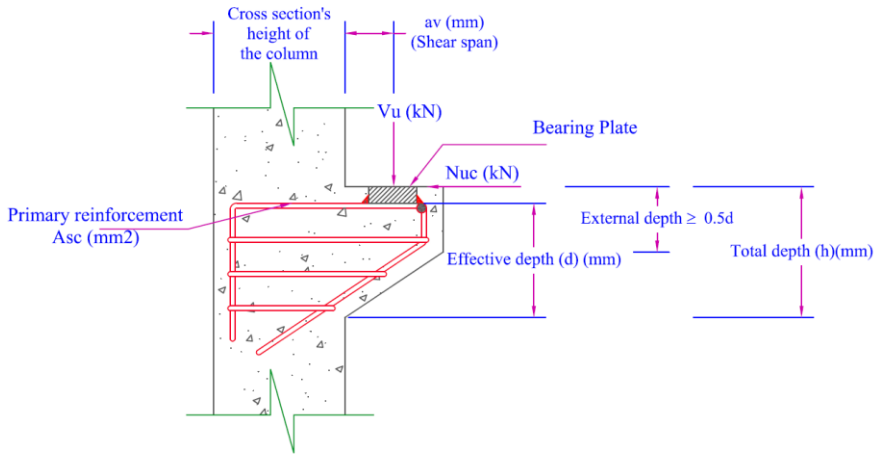

Fig. 1 Corbel’s design variables

technique involved the formulation of the optimal strut-and-tie model, relying on smooth evolutionary optimization with stress constraints. A comparison study between the optimized outputs and those of previous works demonstrates the validity of the proposed optimization analysis. Mello *et al.* (2021) developed an open-source library of RC membrane and used it for the analysis of RC membrane elements, like walls, beams, corbels, shells, and bridges, via the Modified Compression Field Theory and the Disturbed Stress Field Model (DSFM). This model was optimized to predict post-concrete cracking results. A new relationship was formulated accordingly to minimize the impact of the compression softening of concrete in the elements while resisting tensile stresses.

Recently, machine learning techniques such as genetic programming, Artificial Neural Networks (ANN), an adaptive neuro-fuzzy inference system, and support vector machines have been used in the modeling of concrete properties based on optimization and prioritization approaches (Golafshani *et al.* 2020). The application of ANN for the task of prediction of RC corbels’ strength is limited in the previous works. Kumar and Barai (2010) presented an artificial neural network model relying on developed semi-empirical equations to calculate the shear strength of steel-fiber-reinforced concrete corbels. These members were fabricated without using shear reinforcement, and they were tested under the effect of vertical loading. The analysis was performed utilizing Backpropagation ANN and Levenberg-Marquardt algorithm coded in MATLAB. Calculations were in agreement with the available experimental data and results of some previously proposed models. The versatility of the proposed ANN was confirmed via formulation relationships among many variables for the complex physical expressions. According to the aforementioned comprehensive literature review, it can be demonstrated that more research is essential in finding the optimized design of the RC corbels considering the ANN technique. In the other word, while ANNs and other machine learning techniques have been widely used in modeling concrete properties and other aspects of civil engineering, this study uniquely focuses on the application of ANNs to optimize the design of RC corbels. Previously, the use of ANN in this specific area has been limited, marking this endeavor as a novel approach to leveraging computational intelligence for structural engineering design.

This research introduces innovative ANN models for optimizing RC corbel designs, enhancing accuracy, efficiency, and cost-effectiveness in structural engineering. Validated against building codes, these models prove reliable across varying conditions, laying a foundation for future advancements in computational design tools. By integrating machine learning, the study marks a significant step towards more data-driven and economical construction practices.

The aim of present study is represented in leveraging advanced machine learning techniques to improve the structural design of RC corbels, making the process more efficient, accurate, and cost-effective, with a broader impact on construction practices and future research in the field. Overall, the novelty of this study is attributed to its pioneering application of ANN techniques to the specific challenge of RC corbel design optimization, the development of accessible and accurate mathematical models, and the comprehensive approach to incorporating a wide range of data and factors into the design process.

2. Corbel’s design problem and its formulation

The design of corbels is mainly dependent on the concrete’s strength, the steel bars’ yielding stress, the applied loading, and the corbel’s location with respect to its support. Referring to the ACI 318-19 (2019) applications and calculations, a common structural layout of corbels can be provided as depicted in Fig. 1. This design standard recommended the values of the aforementioned control parameters or variables, which are listed in Table 1 and adopted in the present optimized design prediction. Consequently, 1584 RC corbels were designed optimally using the pattern search technique (Rios-Coelho *et al.* 2010, Beigi and Maroosi 2018, Rizk-Allah and Hassanien 2022). The support of the corbel was assumed to be restrained against lateral movement, where a horizontal force of at least 20 percent of the vertical shear should be applied to this structure.

Table 1 The adopted magnitudes of the main variables used in the optimized design of RC corbels

Design parameter	Commonly used value
Yield stress of the reinforcing steel (MPa)	276, 345, 420 and 500
Compressive strength for the concrete (MPa)	20, 25, 30, 35, 40 and 45
Location of the vertical load from the face of the support (mm)	200, 220, 240, 260, 280 and 300
Applied load (kN)	150, 170, 190, 210, 230, 250, 270, 290, 310, 330 and 350

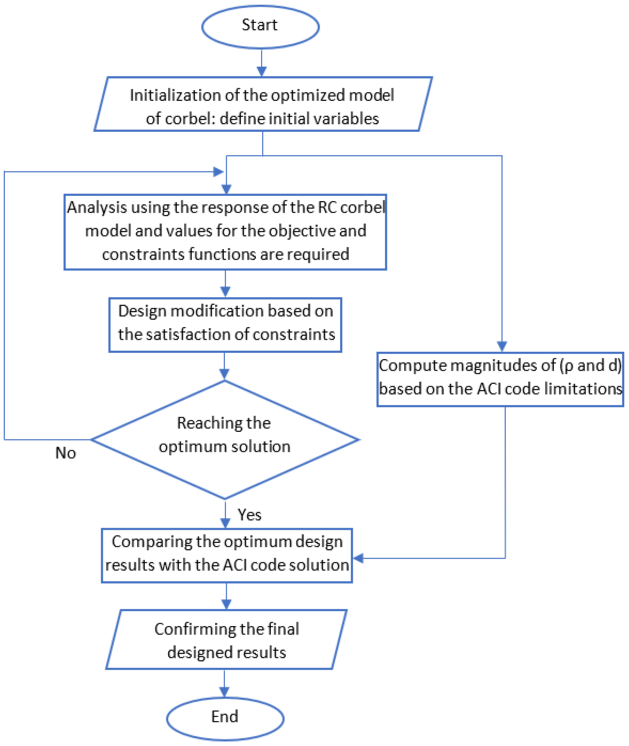

Fig. 2 Optimization process flowchart for RC corbel analysis coded in MATLAB

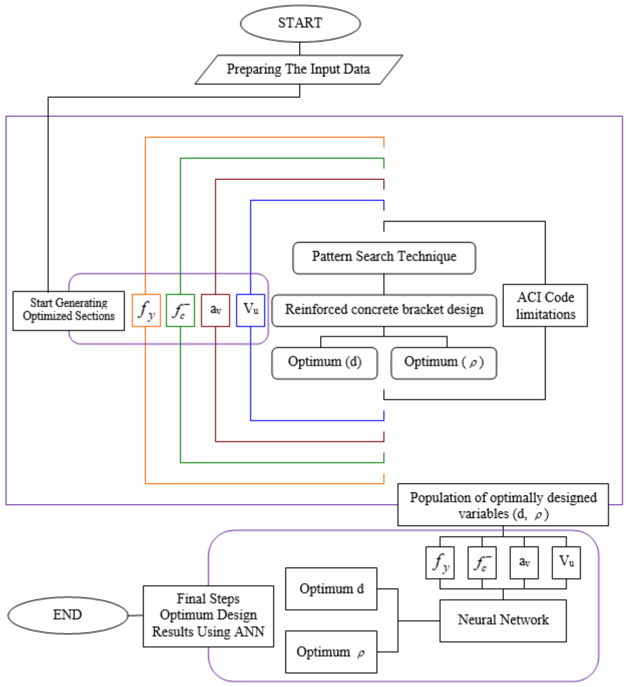

Fig. 3 The schematic structure of the current hybrid analysis system (optimization and neural network approaches)

The pattern search optimization technique is one of the straightforward, derivative-free approaches that was utilized in solving complicated engineering problems that did not comply with the limitations of the standard optimization procedures (Beigi and Maroosi 2018, Rizk-Allah and Hassanien 2022). The advantages of this technique are represented in its calculation efficiency, easiness of implementation, and simplicity in the structure, consequently, it will provide a well-balanced and flexible operator in improving local and global searching existed in pattern search (Lewis *et al.* 2000). In general, this optimization method takes into account the offset of the solution points with respect to the current best solution. Better output between these solutions is accepted and considered as a new best datum for a solution, where iterative analysis around this datum is implementing gain (Rizk-Allah and Hassanien 2022). The adaptation and enhancement of fine local search is provided by pattern search with a well-balanced and flexible operator. A local search optimization, starting with the initial reinforcement ratio (ρ) and optimum effective depth (d) of RC corbels, was utilized in the present study to predict local minimal ρ and d, considering the cost and volume of concrete as given in Fig. 2. This optimization process was coded in MATLAB and complied with that adopted by Lewis *et al.* (2000).

A trading procedure between the design variables took place to find the optimum solutions, which represent the enhanced population of the problem, using the pattern search technique and depending on the cost value represented by the following objective function

$$f_{(x)} = (Volume\ x\ Cost)_{concrete} + (Volume\ x\ Cost)_{steel} \tag{1}$$

Any design procedure should be subjected to a required number of limitations according to the used design code in the field studied. In this study, the ACI 318-19 (2019) was used to provide the needed constraints for the corbel design problem. The pattern search optimum design approach was employed to generate a population of optimum individual solutions for many properties and loading conditions of the RC corbel, this was to find an optimum solution by Artificial Neural Network (ANN) as depicted in Fig. 3. These design limitations are indicated here.

In order to make the cracks of the diagonal tension less steeply inclined, the shear span-to-depth ratio was limited to unity.

$$\frac{a_v}{d} \leq 1.0 \tag{2}$$

Because the design approach has only been validated experimentally, the horizontal force N_{uc} was limited to being no greater than the vertical shear force V_u.

Below the bearing area, a major diagonal tension crack might be propagated to the outer sloping face of the bracket, causing premature failure. To reduce the probability of this happening, the outside edge of the bearing area should have a minimum depth equivalent to half of the effective depth of the bracket.

The cross-sectional dimensions of the concrete and the reinforcing steel should be able to resist the applied bending moment and shear action. As for the applied moment, the design variable was limited to verifying the following design constraint

$$\frac{M_u}{\varphi M_n} \leq 1.0 \tag{3}$$

$$\frac{V_u a_v + N_{uc}(h-d)}{\varphi f_c^- b d^2(\omega - 0.59\omega^2)} \leq 1.0 \tag{4}$$

where

$$\omega = \frac{\rho . f_y}{f_c^-} \tag{5}$$

The optimum reinforcement ratio is used to calculate the reinforcing steel area (A_f) that is sufficient to resist the applied moment.

where

$$A_f = \rho . b_w . d \tag{6}$$

φ: Shear reduction factor = 0.75

V_u: Vertical shear force

N_{uc}: Horizontal tensile force

a_v: Shear span measured from the face of the support

h: Total depth of the bracket

d: Effective depth of the bracket

f_y: Yield stress of the reinforcing steel

f_c^-: Compressive strength of concrete

b_w: Width of the bracket

In addition, the applied factored shear force was limited to the maximum shearing capacity of the section as follows

$$\left.\begin{array}{l} \frac{V_u/\varphi}{0.2 f_c^- b_w d} \leq 1.0 \\ \frac{V_u/\varphi}{(3.3+0.08 f_c^-) b_w d} \leq 1.0 \\ \frac{V_u/\varphi}{11 b_w d} \leq 1.0 \end{array}\right\} \tag{7}$$

Since the applied force was restrained against lateral movement, an equality constraint was used to limit the factored horizontal tensile force to one-fifth of the factored vertical shear.

In order to provide sufficient reinforcing steel to resist the horizontal tensile force, the following restraint was used

$$\frac{N_{uc}}{\varphi A_n f_y} \leq 1.0 \tag{8}$$

where

A_n: The reinforcing steel to resist the factored tensile horizontal force

According to the ACI code, the primary tension reinforcement (A_{sc}) shall not be less than the following constraints

$$\frac{A_{sc}}{\frac{2}{3}A_{vf} + A_n} \geq 1.0 \tag{9}$$

where

$$A_{sc} = A_f + A_n \tag{10}$$

$$A_{vf} = \frac{V_u}{\varphi 1.4 f_y} \tag{11}$$

To prevent the possibility of a sudden failure, a minimum amount of reinforcement is required under the action of flexural moments, as follows

$$\frac{A_{sc}/b_w d}{0.04(\frac{f_c^-}{f_y})} \geq 1.0 \tag{12}$$

For architectural considerations, the depth of the optimum brackets was limited between upper and lower values as follows

$$\left.\begin{array}{l} \frac{d}{200.mm} \geq 1.0 \\ \frac{d}{500.mm} \leq 1.0 \end{array}\right\} \tag{13}$$

Finally, limit the reinforcement ratio to a maximum value as follows

$$\frac{A_{sc}/b_w d}{0.85.\beta 1.(\frac{f_c^-}{f_y}).\frac{3}{7}} \leq 1.0 \tag{14}$$

3. Optimized outputs for corbel design

Table A1 (see Appendix A) shows the design results of randomly selected input data from the optimized designed sections, these data were used to design the same brackets utilizing ACI code. These input data, for ANN, were generated from pattern search approach as illustrated in the Fig. 3. According to the used data, the design outputs were compared for the same material's mechanical properties and loading conditions. The optimum sections followed a compromising procedure (i.e., reducing the effective depth and raising the reinforcement ratio, and vice versa) in order to get the cheapest and most reliable resisting sections.

Fig. 4 compares the cost for the optimally designed section of corbel with the sections designed using ACI code, this was performed according to the local prices, or Iraqi Dinar currency (ID), per cubic volume of the used materials. It is clearly seen that the optimum sections were designed with lower cost values, depending on the material used in the reinforced concrete brackets, compared to ACI calculations.

4. Developed an artificial neural network method

ANN is an artificial intelligence approach to simulating the behavior of the nervous system of the human brain (Abdul-Razzak and Yousif (2013), Kotsovou *et al.* 2017). This process is configured for structural engineering in terms of data classification, prediction of measurements,

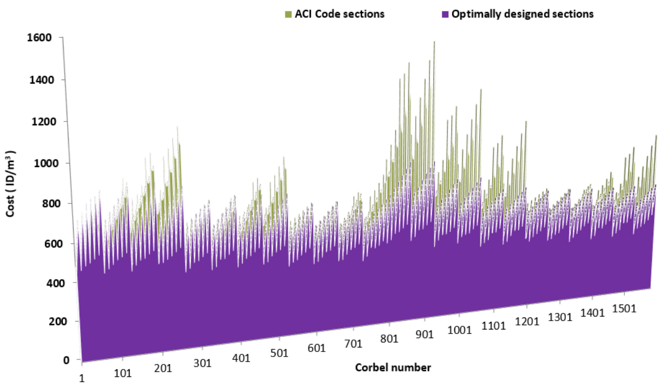

Fig. 4 Cost of the designed corbels using the pattern search technique and the ACI code

Table 2 The range of input and output data

Input	Minimum	Maximum
Yield strength of steel (*fy*) in MPa	276	500
Compressive strength of concrete (*fc'*) in MPa	20	45
Shear span (*av*) in mm	200	300
Vertical applied load (*Vu*) in kN	150	350
Output		
Reinforcement ratio (ρ%)	0.004648	0.025648
The effective depth of corbel (*d*) in mm	200.519	377.3174

and recognition of patterns using training operations on data. The sort of computation performed by ANN, the transmission of activities throughout the neural network, and the joining manner of neurons are highly affected by the effectiveness of the neural network (Kotsovou *et al.* 2017). Thus, an algorithm should be developed for ANN to analyze structural engineering problems that are too complicated to be solved by regular analytical methods. Multilayer ANN is a commonly utilized form of the network because of its simple implementation with respect to the neuron layers, viz., output, input, and hidden layers, which are connected to each other via weighted magnitudes referring to the importance of each input in the prediction process of outputs. In the present work, the Leven Berg-Marquardt (LM) method was used. This approach is based on the conjugate gradient algorithm. The LM algorithm is faster than the traditional gradient descent type of algorithm for training ANNs. This algorithm begins training with the steepest gradient in the first iteration. An ANN was developed for the optimum design of RC corbels using the LM algorithm and 1568 sets of data (see Appendix A), which are the outcomes of the optimized solution for the corbel's design. The range of the input and output is listed in Table 2. 70 percent of these data were selected randomly in the process, while 15 percent of the data were adopted in each testing and validation operation.

The input data were scaled, and the corresponding predicted values should be unscaled. The scaling was implemented with a range of [-1, 1]. Accordingly, the scaling of training data was performed as follows

$$y = \frac{2(x - x_{max})}{(x_{max} - x_{min})} + 1 \quad (15)$$

The output data were scaled between the interval [0, 1] as follows

$$y = \frac{(x - x_{min})}{(x_{max} - x_{min})} \quad (16)$$

During model training, a number of neural network architectures were examined by changing the number of neurons in the hidden layer and the coefficients of the training function to reach a stable and appropriate model. Two forms of activation function were used, namely: Tan-Sigmoid for the hidden layer and Log-Sigmoid for the output layer. Consequently, two models of ANN were developed, viz., a model for predicting the optimum reinforcement ratio of a corbel and a model to compute the optimum corbel depth. In the first ANN model, four inputs were adopted, namely, *fy*, *fc'*, *Av*, and *Vu*, while in the second model, five inputs were selected as those used in the first model in addition to the reinforcement ratio. Figs. 5 and 6 show the architecture of the proposed ANN models. The matching between the predicted values of the testing data, using the developed ANN models, and their counterparts (see Appendix A), is given in Fig. 7. This correlation reveals the high accuracy of the proposed ANN models in the prediction of the optimized reinforcement ratio and effective depth of the corbel, considering the computed correlation coefficient (R), which is more than 94%. This indicates that the model has been well-trained, as the predicted values are close to the actual ones.

5. The proposed mathematical ANN models

The developed ANN can be expressed in the form of

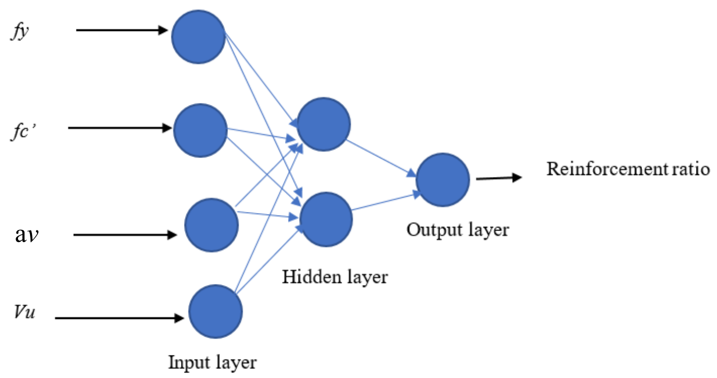

Fig. 5 Architecture of the proposed ANN for reinforcement ratio

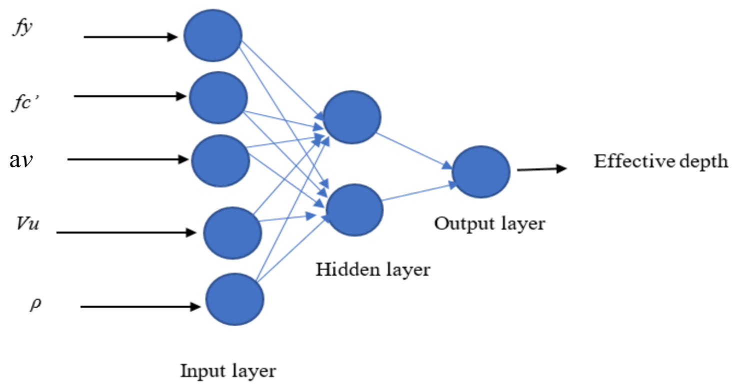

Fig. 6 Architecture of the proposed ANN for the effective depth

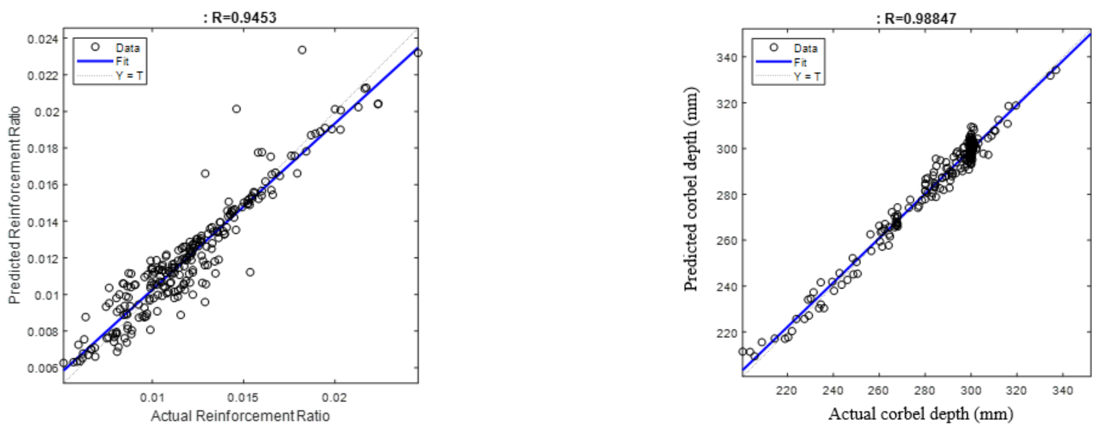

(a) (b)

Fig. 7 Comparison between the actual and predicted values of reinforcement ratio and effective depth of corbels

mathematical models using the weights of the links between the neurons and the activation function used. In the present endeavor, an empirical model was formulated to estimate the optimum reinforcement ratio of RC corbels as follows

$$\rho = 0.004648 + 0.021X \tag{17}$$

where

$$X = \frac{1}{1+e^{-XX}} \tag{18}$$

$$XX = 1.2601 - 3.1739XX1 + 1.0384XX2 \tag{19}$$

$$XX1 = \frac{2}{1+e^{-2X1}} - 1 \tag{20}$$

$$XX2 = \frac{2}{1+e^{-2X2}} - 1 \tag{21}$$

$$X1 = 1.4824 + 0.5670y1 + 0.0125y2 - 0.2779y3 - 0.5638y4 \tag{22}$$

$$X2 = 1.4450 - 0.5710y1 - 0.03324y2 - 0.2210y3 + 1.3226y4 \tag{23}$$

$$y1 = 0.00893(fy - 276) - 1 \tag{24}$$

$$y2 = 0.08(fc - 20) - 1 \tag{25}$$

$$y3 = 0.02(Av - 200) - 1 \quad (26)$$

$$y4 = 0.01(Vu - 150) - 1 \quad (27)$$

The second empirically formulated model is devoted to predicting the effect depth of the corbel as follows

$$d = 200.519 + 176.8Y \quad (28)$$

where

$$Y = \frac{1}{1+e^{-XXX}} \quad (29)$$

$$XXX = -289.908 - 173.2216XX11 - 470.3921XX22 \quad (30)$$

$$XX11 = \frac{2}{1+e^{-2X11}} - 1 \quad (31)$$

$$XX22 = \frac{2}{1+e^{-2X22}} - 1 \quad (32)$$

$$X11 = 1.1478 - 0.2454y1 - 0.0228y2 + 0.0861y3 + 0.18820 * y4 - 0.0954y5 \quad (33)$$

$$X22 = -1.5564 + 0.2007y1 + 0.01886y2 - 0.0738y3 - 0.1636y4 + 0.1136y5 \quad (34)$$

$$y5 = 95.2381 * (\rho - 0.004648) - 1 \quad (35)$$

The important factor for each input was determined as given in Figs. 8 and 9. It is demonstrated that the applied load and yield strength of steel bars are more effective in the calculation of ρ and d respectively with respect to the important factor.

The advantage of using neural network technique in the present optimization process lies in ANN capacity to formulate models of complex mathematical relationships and compute effective outputs in various RC corbel's problem domains.

6. Validation of ANN mathematical models

The verification of the present ANN mathematical models was performed for the randomly selected corbel examples (Table 2), where the predicted values of reinforcement ratio and effect depth of the corbel as predicted by these models and ACI code were compared with the optimum magnitudes of the pattern search optimization technique. Figs. 10 and 11 refer to the accuracy of the proposed ANN models in the prediction of the optimized reinforcement ratio and effective depth of the RC corbel by comparing them with ACI calculations. This process reveals that the predicted values, using ANN models, have considerable reliability based on the agreement between these values and the optimum data, which were found by the pattern search optimization technique for the selected corbels. Fig. 12 can be utilized for further confirmation of the validity of the proposed ANN models in terms of cost reduction of the optimized design of the selected thirty-one corbels compared to the

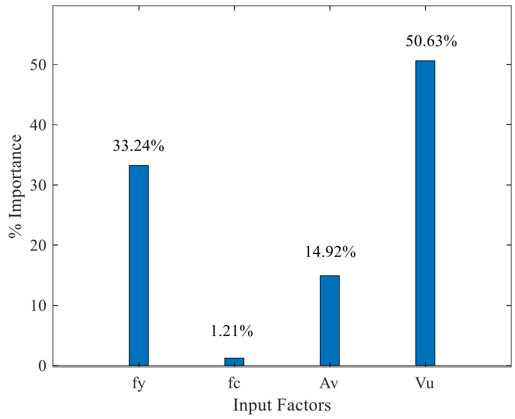

Fig. 8 Importance of the inputs of the proposed models for ρ

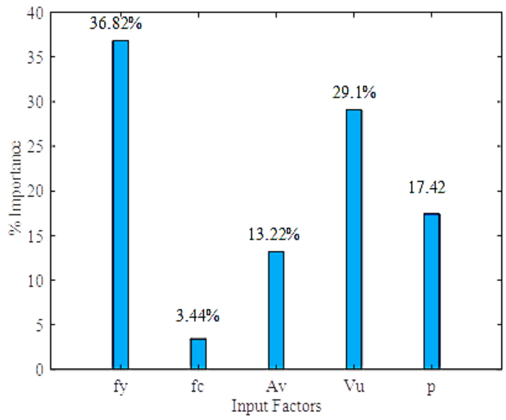

Fig. 9 Importance of the inputs of the proposed models for d

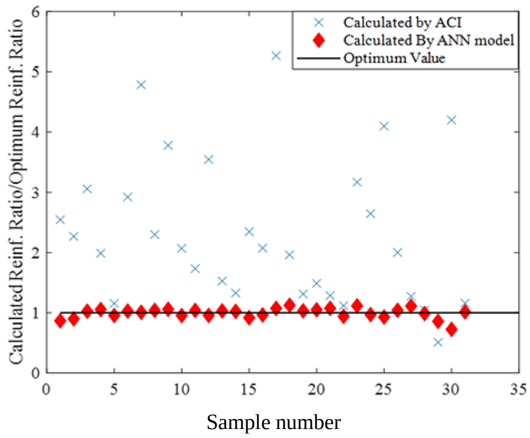

Fig. 10 Comparison between the proposed ANN model and ACI method in terms of reinforcement ratio of corbels

ACI design method. The unique feature of this study compared to previous research lies in employing an optimized database to formulate ANN models.

7. Parametric investigation

Four main parameters were selected in the proposed mathematical formulations (Eqs. (17) and (28)) for the optimum reinforcement ratio and effect depth of a corbel.

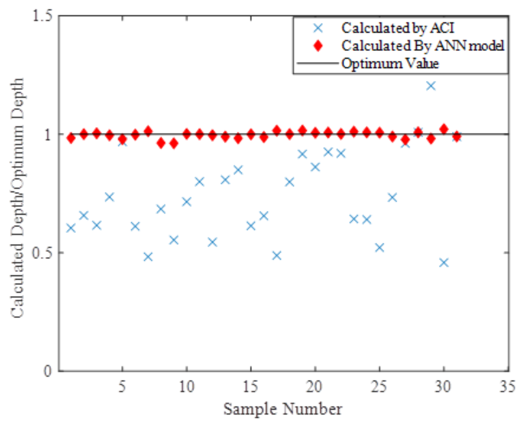

Fig. 11 Comparison between the proposed ANN model and ACI method in terms of effective depth of corbels

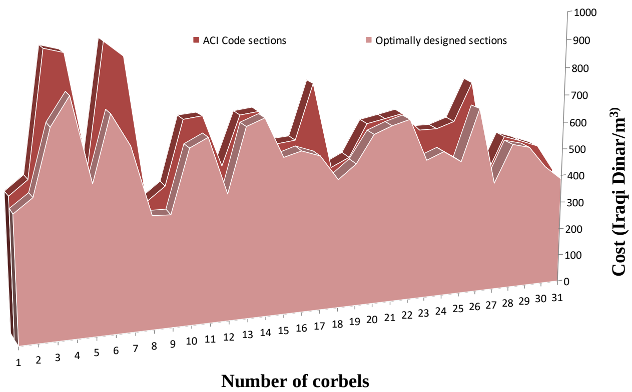

Fig. 12 Comparison between the proposed optimized ANN approach and the ACI method of corbel design in terms of concrete cost

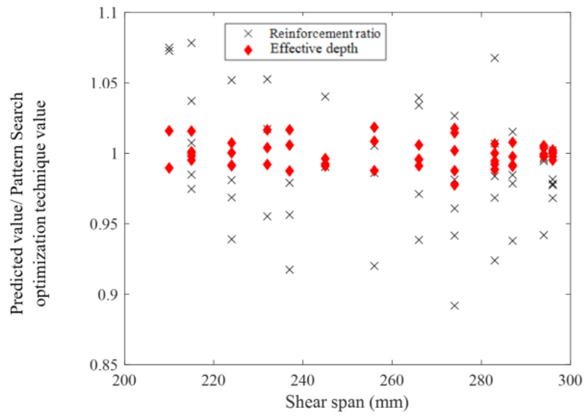

Fig. 13 Reliance of the proposed Eqs. (17) and (28) on the shear span of the corbel

The contribution and role of these variables are implied in the aforementioned method in specific forms. Hence, the computation of the fitness of these mathematical models is essential according to each of these parameters. Figs. 13-16 illustrate the variance of the ratio of the predicted output using the above-mentioned equations, which are calculated by ANN algorithms taking into account the independent variables. In general, no outstanding dependence is observed of the predicted reinforcement ratio on input

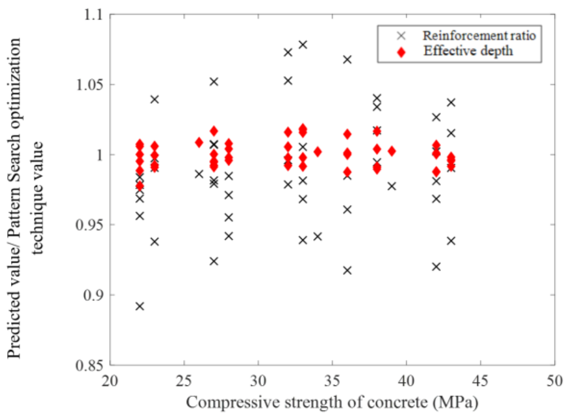

Fig. 14 Reliance of the proposed Eqs. (17) and (28) on the concrete compressive strength

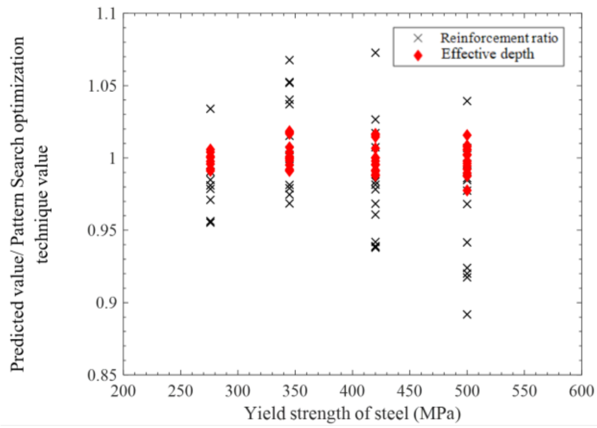

Fig. 15 Reliance of the proposed Eqs. (17) and (28) on the steel yield stress

parameters regardless of their scattering with a wide range. This indicates that consideration of these variables will effectively improve the fitness of the proposed neural network models using the weights assigned to parameters during analysis.

8. Conclusions

Two empirical ANN mathematical models were formulated in the present study to predict the optimum reinforcement ratio and effective depth of the RC corbel. More than one thousand five hundred of data were compiled, from the analysis of corbel samples using the pattern search optimization technique and employed in this computational artificial neural solution. Five design variables were selected to formulate reliable and simple ANN mathematical models. These formulations were applicable for the calculation of the optimized reinforcement ratio and effect depth of the corbels, considering the cost factor. The validity of the proposed ANN models was confirmed by comparison between their outcomes and those for a building code. The justification of the independent variables of the proposed ANN expressions was conducted through a parametric investigation. This process demonstrated the reliability of these ANN models,

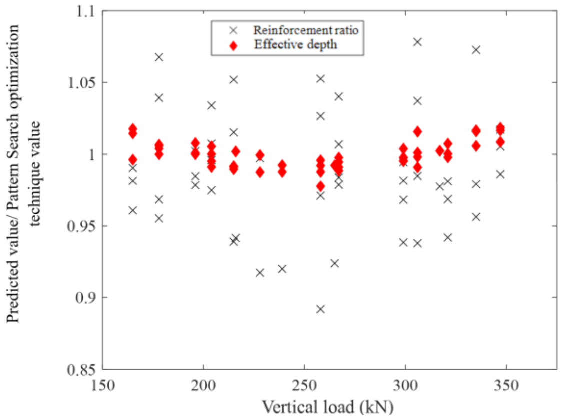

Fig. 16 Reliance of the proposed Eqs. (17) and (28) on the applied vertical load on a corbel

though there is a broad range of differences in the adopted independent parameters. Thus, it is proved that the integration of these parameters in the proposed neural models is successful. The stability and simplicity of the proposed ANN mathematical models point out that they are suitable for the task of optimizing the structural design of RC corbels.

References

ACI 318-19 (2019), American Concrete Institute Building Code Requirements for Structural Concrete, American Concrete Institute, Farmington Hills, MI, USA.

Abdul-Razzak, A.A. and Ali, A.A.M. (2011), "Modelling and numerical simulation of high strength fibre reinforced concrete corbels", *Appl. Math. Model.*, **35**(6), 2901-2915. https://doi.org/10.1016/j.apm.2010.11.073.

Abdul-Razzaq, K.S. and Dawood, A.A. (2020), "Corbel strut and tie modeling-Experimental verification", *Struct.*, **26**, 327-339. https://doi.org/10.1016/j.istruc.2020.04.021.

Abdul-Razzak, A.A. and Yousif, S.T. (2013), "Artificial neural networks model for predicting nonlinear response of rectangular plates", *The Second Scientific Engineering Conference*, Mosul, Iraq, November.

Abu-Obaida, A., El-Maaddawy, T. and El-Ariss, B. (2020), "Numerical simulation of double-sided concrete corbels internally-reinforced with GFRP bars", *Compos. Part C: Open Access*, **2**, 100040. https://doi.org/10.1016/j.jcomc.2020.100040.

Adrija, D., Geevar, I., Menon, D. and Prasad, M. (2021), "Strength assessment of RC deep beams and corbels", *Struct. Eng. Mech.*, **77**(2), 273-291. https://doi.org/10.12989/sem.2021.77.2.273.

Al-Kamaki, Y.S.S., Hassan, G.B. and Alsofi, G. (2018), "Experimental study of the behaviour of RC corbels strengthened with CFRP sheets", *Case Stud. Constr. Mater.*, **9**, e00181. https://doi.org/10.1016/j.cscm.2018.e00181.

Al-Shaarbaf, I.A., Al-Azzawi, A.A. and Farahan, R.S. (2015), "Experimental investigation on the behavior of reinforced concrete corbels under repeated loadings", *J. Eng. Sustainab. Develop.*, **19**(4), 126-147.

Almeida, V.S., Simonetti, H.L. and Neto, L.O. (2013), "Comparative analysis of strut-and-tie models using smooth evolutionary structural optimization", *Eng. Struct.*, **56**, 1665-1675. https://doi.org/10.1016/j.engstruct.2013.07.007.

Amir, O. (2013), "A topology optimization procedure for reinforced concrete structures", *Comput. Struct.*, **114**, 46-58. https://doi.org/10.1016/j.compstruc.2012.10.011.

Asnake, F. (2016), "A finite element method based analysis of corbels", Master's Thesis, Addis Ababa University, Addis Ababa, Ethiopia.

Beigi, A.M. and Maroosi, A. (2018), "Parameter identification for solar cells and module using a hybrid firefly and pattern search algorithms", *Solar Energy*, **171**, 435-446. https://doi.org/10.1016/j.solener.2018.06.092.

Bruggi, M. (2009), "Generating strut-and-tie patterns for reinforced concrete structures using topology optimization", *Comput. Struct.*, **87**(23-24), 1483-1495. https://doi.org/10.1016/j.compstruc.2009.06.003.

Campione, G. (2009), "Flexural response of FRC corbels", *Cement Concrete Compos.*, **31**(3), 204-210. https://doi.org/10.1016/j.cemconcomp.2009.01.006.

Campione, G., La Mendola, L. and Mangiavillano, M.L. (2007), "Steel fiber-reinforced concrete corbels: Experimental behavior and shear strength prediction", *ACI Struct. J.*, **104**(5), 570. https://doi.org/10.14359/18859.

Campione, G., La Mendola, L. and Papia, M. (2005), "Flexural behaviour of concrete corbels containing steel fibers or wrapped with FRP sheets", *Mater. Struct.*, **38**(6), 617-625. https://doi.org/10.1007/BF02481593.

Canha, R.M.F., Kuchma, D.A., El Debs, M.K. and de Souza, R.A. (2014), "Numerical analysis of reinforced high strength concrete corbels", *Eng. Struct.*, **74**, 130-144. https://doi.org/10.1016/j.engstruct.2014.05.014.

Chetchotisak, P., Teerawong, J. and Yindeesuk, S. (2022), "Modified interactive strut-and-tie modeling of reinforced concrete deep beams and corbels", *Struct.*, **45**, 284-298. https://doi.org/10.1016/j.istruc.2022.08.116.

Chiniforush, A.A., Gharehchaei, M., Nezhad, A.A., Castel, A., Moghaddam, F., Keyte, L., Hocking, D. and Foster, S. (2021), "Minimising risk of early-age thermal cracking and delayed ettringite formation in concrete-A hybrid numerical simulation and genetic algorithm mix optimisation approach", *Constr. Build. Mater.*, **299**, 124280. https://doi.org/10.1016/j.conbuildmat.2021.124280.

de Lima Araújo, D., Coelho, S.A., de Almeida, S.R.M. and El Debs, M.K. (2021), "Computational modelling and analytical model for two-step corbel for precast concrete system", *Eng. Struct.*, **244**, 112699. https://doi.org/10.1016/j.engstruct.2021.112699.

DeRousseau, M., Kasprzyk, J. and Srubar Iii, W. (2018), "Computational design optimization of concrete mixtures: A review", *Cement Concrete Res.*, **109**, 42-53. https://doi.org/10.1016/j.cemconres.2018.04.007.

Fattuhi, N.I. and Hughes, B.P. (1989), "Ductility of reinforced concrete corbels containing either steel fibers or stirrups", *Struct. J.*, **86**(6), 644-651. https://doi.org/10.14359/2660.

Foster, S.J., Powell, R.E. and Selim, H.S. (1996), "Performance of high-strength concrete corbels", *Struct. J.*, **93**(5), 555-563. https://doi.org/10.14359/9714.

Gao, D. and Zhang, J. (2010), "Finite element analysis of shear behaviors for steel fiber reinforced concrete corbels by ANSYS", *2010 Second International Conference on Computer Modeling and Simulation*, Hainan, China, January.

Golafshani, E.M., Behnood, A. and Arashpour, M. (2020), "Predicting the compressive strength of normal and High-Performance Concretes using ANN and ANFIS hybridized with Grey Wolf Optimizer", *Constr. Build. Mater.*, **232**, 117266. https://doi.org/10.1016/j.conbuildmat.2019.117266.

Huang, Y., Zhang, J., Ann, F.T. and Ma, G. (2020), "Intelligent mixture design of steel fibre reinforced concrete using a support vector regression and firefly algorithm based multi-objective optimization model", *Constr. Build. Mater.*, **260**, 120457.

https://doi.org/10.1016/j.conbuildmat.2020.120457.
İpek, S., Güneyisi, E.M., Mermerdaş, K. and Algın, Z. (2021), "Optimization and modeling of axial strength of concrete-filled double skin steel tubular columns using response surface and neural-network methods", *J. Build. Eng.*, **43**, 103128. https://doi.org/10.1016/j.jobe.2021.103128.
Ivanova, I. and Assih, J. (2015), "Static and dynamic experimental study of strengthened inforced short concrete corbel by using carbon fabrics, crack path in shear zone", *Fract. Struct. Integr.*, **9**(34), 1. https://doi.org/10.3221/IGF-ESIS.34.09.
Kotsovou, G.M., Cotsovos, D.M. and Lagaros, N.D. (2017), "Assessment of RC exterior beam-column Joints based on artificial neural networks and other methods", *Eng. Struct.*, **144**, 1-18. https://doi.org/10.1016/j.engstruct.2017.04.048.
Kumar, S. and Barai, S. (2010), "Neural networks modeling of shear strength of SFRC corbels without stirrups", *Appl. Soft Comput.*, **10**(1), 135-148. https://doi.org/10.1016/j.asoc.2009.06.012.
Lachowicz, M. and Nagrodzka-Godycka, K. (2016), "Experimental study of the post tensioned prestressed concrete corbels", *Eng. Struct.*, **108**, 1-11. https://doi.org/10.1016/j.engstruct.2015.11.007.
Lewis, R.M., Torczon, V. and Trosset, M.W. (2000), "Direct search methods: Then and now", *J. Comput. Appl. Math.*, **124**(1-2), 191-207. https://doi.org/10.1016/S0377-0427(00)00423-4.
Lu, W.Y. and Lin, I.J. (2009), "Behavior of reinforced concrete corbels", *Struct. Eng. Mech.*, **33**(3), 357-371. https://doi.org/10.12989/sem.2009.33.3.357.
Manzoli, O.L., Oliver, J., Diaz, G. and Huespe, A.E. (2008), "Three-dimensional analysis of reinforced concrete members via embedded discontinuity finite elements", *IBRACON Struct. Mater. J.*, **1**, 58-83. https://doi.org/10.1590/S1983-41952008000100004.
Mattock, A.H., Chen, K. and Soongswang, K. (1976), "The behavior of reinforced concrete corbels", *PCI J.*, **21**(2), 52-77.
Mello, A.F.A., Trautwein, L.M., Almeida, L.C. and Souza, R.A. (2021), "Development of an open source library for reinforced concrete membrane element analysis", *Struct.*, **34**, 4882-4891. https://doi.org/10.1016/j.istruc.2021.10.043
Mohammad, A.K.Q. and Al-Shamaa, M.F.K. (2018), "Experimental study of behavior of reactive powder concrete strengthening by NSM-CFRP corbels", *Civil Eng. J.*, **4**(5), 980-992. http://doi.org/10.28991/cej-0309150.
Mozaffari, S., Akbarzadeh, M. and Vogel, T. (2020), "Graphic statics in a continuum: Strut-and-tie models for reinforced concrete", *Comput. Struct.*, **240**, 106335. https://doi.org/10.1016/j.compstruc.2020.106335.
Nikbakht, S., Kamarian, S. and Shakeri, M. (2019), "A review on optimization of composite structures Part II: Functionally graded materials", *Compos. Struct.*, **214**, 83-102. https://doi.org/10.1016/j.compstruct.2019.01.105.
Ozden, S. and Atalay, H.M. (2011), "Strengthening of reinforced concrete corbels with GFRP overlays", *Sci. Eng. Compos. Mater.*, **18**(1-2), 69-77. https://doi.org/10.1515/secm.2011.009.
Özkal, F. Mehmet. and Uysal, H. (2017), "Reinforcement detailing of a corbel via an integrated strut-and-tie modeling approach", *Comput. Concrete*, **19**(5), 589-597. https://doi.org/10.12989/cac.2017.19.5.589.
Parol, J., Al-Qazweeni, J. and Salam, S.A. (2018), "Analysis of reinforced concrete corbel beams using strut and tie models", *Comput. Concrete,* **21**(1), 95-102. https://doi.org/10.12989/cac.2018.21.1.095.
Pierott, R., Hammad, A.W., Haddad, A., Garcia, S. and Falcón, G. (2021), "A mathematical optimisation model for the design and detailing of reinforced concrete beams", *Eng. Struct.*, **245**, 112861. https://doi.org/10.1016/j.engstruct.2021.112861.
Prasad, H.R., Channakeshava, C., Prasad, B.R. and Iyengar, K.S.R. (1993), "Nonlinear finite element analysis of reinforced concrete corbel", *Comput. Struct.*, **46**(2), 343-354. https://doi.org/10.1016/0045-7949(93)90199-N.
Ridha, M.M., Al-Shafi'i, N.T. and Hasan, M.M. (2017), "Ultra-high performance steel fibers concrete corbels: Experimental investigation", *Case Stud. Constr. Mater.*, **7**, 180-190. https://doi.org/10.1016/j.cscm.2017.07.004.
Rios-Coelho, A.C., Sacco, W.F. and Henderson, N. (2010), "A Metropolis algorithm combined with Hooke-Jeeves local search method applied to global optimization", *Appl. Math. Comput.*, **217**(2), 843-853. https://doi.org/10.1016/j.amc.2010.06.027.
Rizk-Allah, R.M. and Hassanien, A.E. (2022), "A hybrid equilibrium algorithm and pattern search technique for wind farm layout optimization problem", *ISA Trans.*, **132**, 402-418. https://doi.org/10.1016/j.isatra.2022.06.014
Shakir, Q.M. (2020), "Response of innovative high strength reinforced concrete encased-composite corbels", *Struct.*, **25**, 798-809. https://doi.org/10.1016/j.istruc.2020.03.056.
Smarslik, M., Ahrens, M.A. and Mark, P. (2019), "Toward holistic tension-or compression-biased structural designs using topology optimization", *Eng. Struct.*, **199**, 109632. https://doi.org/10.1016/j.engstruct.2019.109632.
Souza, R.A.D., Trautwein, L.M. and Ferreira, M.d.P. (2019), "Reinforced concrete corbel strengthened using carbon fiber reinforced polymer (CFRP) sheets", *J. Compos. Sci.*, **3**(1), 26. https://doi.org/10.3390/jcs3010026
Strauss, A., Mordini, A. and Bergmeister, K. (2006), "Nonlinear finite element analysis of reinforced concrete corbels at both deterministic and probabilistic levels", *Comput. Concrete*, **3**(2), 123-144. https://doi.org/10.12989/cac.2006.3.2/3.123.
Syroka, E., Bobiński, J. and Tejchman, J. (2011), "FE analysis of reinforced concrete corbels with enhanced continuum models", *Finite Elem. Anal. Des.*, **47**(9), 1066-1078. https://doi.org/10.1016/j.finel.2011.03.022.
Torres, F. (1998), "Theoretic-experimental analysis of reinforced concrete corbels", MSc Thesis, Sao Paulo University, Sao Carlos, Brazil.
Yong, Y., McCloskey, D.H. and Nawy, E.G. (1985), "Reinforced corbels of high-strength concrete", *Spec. Publ.*, **87**, 197-212. https://doi.org/10.14359/6530.

CC

Appendix A

Table A1 Optimum design of RC corbels

Sample No.	*d* (mm)	*ρ*	*Vu* (kN)	*av* (mm)	*fc'* (MPa)	*fy* (MPa)
1	271.35	0.00908	150	200	20	276
2	238.75	0.013393	170	200	20	276
3	293.985	0.009981	190	200	20	276
4	292	0.011316	210	200	20	276
5	294.51	0.012215	230	200	20	276
6	300	0.012884	250	200	20	276
7	300	0.014099	270	200	20	276
8	300	0.015213	290	200	20	276
9	300.0568	0.016327	310	200	20	276
10	299.5	0.017549	330	200	20	276
11	299.496	0.018764	350	200	20	276
12	268	0.010103	150	220	20	276
13	287.4	0.010105	170	220	20	276
14	262.1	0.013635	190	220	20	276
15	293.08	0.012108	210	220	20	276
16	300	0.012769	230	220	20	276
17	301.36	0.013872	250	220	20	276
18	301.32	0.015086	270	220	20	276
19	300.3125	0.01651	290	220	20	276
20	299.988	0.017828	310	220	20	276
21	308.1423	0.018049	330	220	20	276
22	300.698	0.020349	350	220	20	276
23	281.3	0.009917	150	240	20	276
24	280.326	0.011353	170	240	20	276
25	291.77	0.011897	190	240	20	276
26	287.943	0.013549	210	240	20	276
27	300	0.013769	230	240	20	276
28	299.996	0.015084	250	240	20	276
29	299.9948	0.016499	270	240	20	276
30	300	0.017813	290	240	20	276
31	318.889	0.016931	310	240	20	276
32	316.98	0.018453	330	240	20	276
33	299	0.02237	350	240	20	276
34	266.85	0.01181	150	260	20	276
35	283.43	0.011932	170	260	20	276
36	300	0.01204	190	260	20	276
37	299.505	0.013458	210	260	20	276
38	300	0.014869	230	260	20	276
39	299.244	0.016391	250	260	20	276
40	301.4786	0.017584	270	260	20	276
41	308	0.018232	290	260	20	276
42	303.772	0.020187	310	260	20	276
43	299.9897	0.022343	330	260	20	276
44	315.2986	0.021475	350	260	20	276
45	292.218	0.010453	150	280	20	276

Table A1 Continued

Sample No.	*d* (mm)	*ρ*	*Vu* (kN)	*av* (mm)	*fc'* (MPa)	*fy* (MPa)
46	306.862	0.010884	170	280	20	276
47	300	0.01284	190	280	20	276
48	300	0.014354	210	280	20	276
49	300	0.015869	230	280	20	276
50	301.338	0.017272	250	280	20	276
51	299.4853	0.019104	270	280	20	276
52	300	0.020713	290	280	20	276
53	303.054	0.021894	310	280	20	276
54	319.4145	0.020927	330	280	20	276
55	360.07	0.017431	350	280	20	276
56	300.277	0.010609	150	300	20	276
57	300	0.012125	170	300	20	276
58	300	0.01364	190	300	20	276
59	300.6111	0.01525	210	300	20	276
60	309	0.015897	230	300	20	276
61	300.085	0.018583	250	300	20	276
62	300.2441	0.020296	270	300	20	276
63	301.2284	0.021901	290	300	20	276
64	317.7548	0.021142	310	300	20	276
65	336.9865	0.019954	330	300	20	276
66	363.104	0.018204	350	300	20	276
67	235.66	0.01185	150	200	25	276
68	265.31	0.010764	170	200	25	276
69	292.16	0.009994	190	200	25	276
70	296.714	0.010779	210	200	25	276
71	282.9445	0.013018	230	200	25	276
72	300	0.012784	250	200	25	276
73	299.9985	0.013799	270	200	25	276
74	299.5	0.014918	290	200	25	276
75	297.104	0.01636	310	200	25	276
76	300.1336	0.017141	330	200	25	276
77	301.1831	0.018143	350	200	25	276
78	248.4626	0.011544	150	220	25	276
79	267.5778	0.011446	170	220	25	276
80	300.873	0.010234	190	220	25	276
81	296.4093	0.011682	210	220	25	276
82	300	0.012569	230	220	25	276
83	300	0.013784	250	220	25	276
84	300.0032	0.014999	270	220	25	276
85	301.5957	0.015997	290	220	25	276
86	299.5	0.017434	310	220	25	276
87	308.52	0.017545	330	220	25	276
88	300.3135	0.019853	350	220	25	276
89	269.2678	0.010594	150	240	25	276
90	299.86	0.009826	170	240	25	276
91	284.4347	0.012251	190	240	25	276
92	300	0.012354	210	240	25	276

Table A1 Continued

Sample No.	*d* (mm)	*ρ*	*Vu* (kN)	*av* (mm)	*fc'* (MPa)	*fy* (MPa)
93	300	0.013569	230	240	25	276
94	301.3157	0.014672	250	240	25	276
95	299.9961	0.016099	270	240	25	276
96	299.803	0.017415	290	240	25	276
97	300.4835	0.018723	310	240	25	276
98	300.3232	0.020039	330	240	25	276
99	303.256	0.021017	350	240	25	276
100	288.466	0.009975	150	260	25	276
101	299.9736	0.010525	170	260	25	276
102	303.5149	0.011616	190	260	25	276
103	300	0.013154	210	260	25	276
104	299.53	0.014573	230	260	25	276
105	305.0216	0.01534	250	260	25	276
106	347.9845	0.012899	270	260	25	276
107	319.2781	0.016525	290	260	25	276
108	299.3689	0.020235	310	260	25	276
109	316.293	0.01936	330	260	25	276
110	310.7121	0.021428	350	260	25	276
111	284.6258	0.010897	150	280	25	276
112	298.25	0.011336	170	280	25	276
113	299.7998	0.012641	190	280	25	276
114	300	0.014054	210	280	25	276
115	299.9935	0.015469	230	280	25	276
116	300.342	0.016981	250	280	25	276
117	299.626	0.018502	270	280	25	276
118	367.64	0.01334	290	280	25	276
119	306.502	0.020657	310	280	25	276
120	299.9994	0.023143	330	280	25	276
121	312.305	0.022709	350	280	25	276
122	300.341	0.010408	150	300	25	276
123	300	0.011925	170	300	25	276
124	300	0.01344	190	300	25	276
125	322.3242	0.012998	210	300	25	276
126	300.71	0.016463	230	300	25	276
127	300.5873	0.017979	250	300	25	276
128	300.1688	0.019697	270	300	25	276
129	300.533	0.021308	290	300	25	276
130	300.2655	0.023025	310	300	25	276
131	300.2393	0.02474	330	300	25	276
132	331.9726	0.021396	350	300	25	276
133	219.388	0.013402	150	200	30	276
134	242.6907	0.012556	170	200	30	276
135	236	0.013593	190	200	30	276
136	284.0566	0.011681	210	200	30	276
137	276	0.013484	230	200	30	276
138	298	0.012802	250	200	30	276
139	300	0.013699	270	200	30	276

Table A1 Continued

Sample No.	d (mm)	ρ	Vu (kN)	av (mm)	fc' (MPa)	fy (MPa)
140	300	0.014713	290	200	30	276
141	300.2359	0.015825	310	200	30	276
142	300	0.016943	330	200	30	276
143	300.9764	0.017945	350	200	30	276
144	273.7637	0.009465	150	220	30	276
145	277.2645	0.010575	170	220	30	276
146	268.2476	0.012681	190	220	30	276
147	283.156	0.012689	210	220	30	276
148	300	0.012469	230	220	30	276
149	300	0.013584	250	220	30	276
150	299.996	0.014799	270	220	30	276
151	300.3548	0.01591	290	220	30	276
152	300.3674	0.017124	310	220	30	276
153	300	0.018343	330	220	30	276
154	300.293	0.019454	350	220	30	276
155	295.6151	0.008834	150	240	30	276
156	268	0.012143	170	240	30	276
157	296.9375	0.011161	190	240	30	276
158	299.7788	0.012156	210	240	30	276
159	293.5186	0.014024	230	240	30	276
160	299.129	0.014692	250	240	30	276
161	298.453	0.016014	270	240	30	276
162	299.994	0.017113	290	240	30	276
163	300.4444	0.018423	310	240	30	276
164	334.4899	0.015977	330	240	30	276
165	301.2641	0.020842	350	240	30	276
166	266.9198	0.01151	150	260	30	276
167	267.2532	0.013049	170	260	30	276
168	295.754	0.012069	190	260	30	276
169	300	0.013054	210	260	30	276
170	300.6698	0.014264	230	260	30	276
171	299.9984	0.015684	250	260	30	276
172	300.0625	0.016998	270	260	30	276
173	321.9199	0.016001	290	260	30	276
174	299.8966	0.019829	310	260	30	276
175	299.9939	0.021143	330	260	30	276
176	306.247	0.021681	350	260	30	276
177	289.4655	0.010469	150	280	30	276
178	284.1477	0.012327	170	280	30	276
179	300	0.01254	190	280	30	276
180	299.515	0.013958	210	280	30	276
181	298.07	0.015485	230	280	30	276
182	297.1265	0.01701	250	280	30	276
183	301.1727	0.017987	270	280	30	276
184	300.433	0.019609	290	280	30	276
185	303.0732	0.020694	310	280	30	276
186	322.48	0.019596	330	280	30	276

Table A1 Continued

Sample No.	*d* (mm)	*ρ*	*Vu* (kN)	*av* (mm)	*fc'* (MPa)	*fy* (MPa)
187	298.2695	0.024479	350	280	30	276
188	301.96	0.0102	150	300	30	276
189	300	0.011825	170	300	30	276
190	300	0.01324	190	300	30	276
191	300	0.014754	210	300	30	276
192	300.1238	0.016268	230	300	30	276
193	311.927	0.016481	250	300	30	276
194	300.1	0.019298	270	300	30	276
195	302.09	0.020592	290	300	30	276
196	304.2	0.021882	310	300	30	276
197	311.5725	0.022311	330	300	30	276
198	300.751	0.025648	350	300	30	276
199	294.2596	0.007642	150	200	35	276
200	244.086	0.012343	170	200	35	276
201	271.9586	0.01135	190	200	35	276
202	263.03	0.013371	210	200	35	276
203	295.7643	0.011804	230	200	35	276
204	299.88	0.012585	250	200	35	276
205	299.9984	0.013599	270	200	35	276
206	300	0.014613	290	200	35	276
207	300.211	0.015626	310	200	35	276
208	300.602	0.016736	330	200	35	276
209	309.61	0.016841	350	200	35	276
210	267.32	0.009907	150	220	35	276
211	258.5	0.012018	170	220	35	276
212	280.4375	0.011582	190	220	35	276
213	299.99	0.011255	210	220	35	276
214	297.4164	0.012591	230	220	35	276
215	299.172	0.013591	250	220	35	276
216	300	0.014699	270	220	35	276
217	299.9922	0.015813	290	220	35	276
218	299.9961	0.016928	310	220	35	276
219	300.8	0.018033	330	220	35	276
220	318.727	0.017137	350	220	35	276
221	261.07	0.01115	150	240	35	276
222	253.6953	0.013358	170	240	35	276
223	299.064	0.010946	190	240	35	276
224	299.931	0.012055	210	240	35	276
225	300	0.013269	230	240	35	276
226	300	0.014484	250	240	35	276
227	300	0.015699	270	240	35	276
228	299.5	0.017018	290	240	35	276
229	301.2997	0.018114	310	240	35	276
230	299.74	0.019546	330	240	35	276
231	299.6563	0.020762	350	240	35	276
232	267.875	0.011303	150	260	35	276
233	288.5747	0.011197	170	260	35	276

Table A1 Continued

Sample No.	d (mm)	ρ	Vu (kN)	av (mm)	fc' (MPa)	fy (MPa)
234	292.185	0.012294	190	260	35	276
235	300	0.012954	210	260	35	276
236	299.5	0.014273	230	260	35	276
237	299.9961	0.015484	250	260	35	276
238	299.1689	0.016907	270	260	35	276
239	300.263	0.018111	290	260	35	276
240	298.135	0.019749	310	260	35	276
241	297.18	0.021276	330	260	35	276
242	299.062	0.022369	350	260	35	276
243	282.6	0.010909	150	280	35	276
244	307.143	0.010583	170	280	35	276
245	300	0.01244	190	280	35	276
246	300	0.013754	210	280	35	276
247	299.996	0.015169	230	280	35	276
248	300.2656	0.016481	250	280	35	276
249	300.178	0.017897	270	280	35	276
250	300	0.019413	290	280	35	276
251	298.3	0.021047	310	280	35	276
252	300	0.022342	330	280	35	276
253	300.902	0.023646	350	280	35	276
254	303.4336	0.010092	150	300	35	276
255	300.0355	0.011725	170	300	35	276
256	300	0.01314	190	300	35	276
257	300.02	0.014654	210	300	35	276
258	300.86	0.015962	230	300	35	276
259	314.31	0.016062	250	300	35	276
260	300	0.019099	270	300	35	276
261	357.904	0.01461	290	300	35	276
262	300.0566	0.022127	310	300	35	276
263	316.2773	0.02136	330	300	35	276
264	330.3262	0.020812	350	300	35	276
265	234.5343	0.009648	150	200	20	345
266	230.2223	0.011503	170	200	20	345
267	265.9154	0.009741	190	200	20	345
268	301.7254	0.008493	210	200	20	345
269	296.9346	0.009696	230	200	20	345
270	291.426	0.01091	250	200	20	345
271	283.2617	0.012656	270	200	20	345
272	296.0675	0.012524	290	200	20	345
273	300	0.013062	310	200	20	345
274	300	0.014034	330	200	20	345
275	300	0.015006	350	200	20	345
276	235.9531	0.010438	150	220	20	345
277	220.3125	0.013788	170	220	20	345
278	231.789	0.014012	190	220	20	345
279	267.9807	0.011619	210	220	20	345
280	269.36	0.0127	230	220	20	345

Table A1 Continued

Sample No.	*d* (mm)	*ρ*	*Vu* (kN)	*av* (mm)	*fc'* (MPa)	*fy* (MPa)
281	291.9926	0.011806	250	220	20	345
282	299.768	0.012221	270	220	20	345
283	300	0.013191	290	220	20	345
284	300	0.014262	310	220	20	345
285	305.25	0.014685	330	220	20	345
286	299.5967	0.01641	350	220	20	345
287	280.4675	0.007978	150	240	20	345
288	271.7578	0.009712	170	240	20	345
289	252.6461	0.012738	190	240	20	345
290	294.8844	0.010335	210	240	20	345
291	300.332	0.010973	230	240	20	345
292	298.0075	0.012261	250	240	20	345
293	300	0.013219	270	240	20	345
294	300.008	0.014291	290	240	20	345
295	299.5579	0.015466	310	240	20	345
296	309.005	0.015552	330	240	20	345
297	300.15	0.017704	350	240	20	345
298	263.9375	0.009664	150	260	20	345
299	305.146	0.008235	170	260	20	345
300	290.61	0.010285	190	260	20	345
301	299.902	0.010704	210	260	20	345
302	299.5525	0.011878	230	260	20	345
303	299.9976	0.013047	250	260	20	345
304	300	0.014219	270	260	20	345
305	300.0023	0.015391	290	260	20	345
306	300.1348	0.016661	310	260	20	345
307	299.9999	0.017934	330	260	20	345
308	316.3532	0.017051	350	260	20	345
309	289.1465	0.008537	150	280	20	345
310	285.0276	0.010137	170	280	20	345
311	280.0237	0.011848	190	280	20	345
312	295.9817	0.011828	210	280	20	345
313	300	0.012675	230	280	20	345
314	302.739	0.013628	250	280	20	345
315	299.1605	0.015325	270	280	20	345
316	299.6617	0.016593	290	280	20	345
317	299.5537	0.017966	310	280	20	345
318	328.06	0.015792	330	280	20	345
319	359.7985	0.013906	350	280	20	345
320	300	0.008488	150	300	20	345
321	309	0.009117	170	300	20	345
322	300.75	0.010928	190	300	20	345
323	300	0.012204	210	300	20	345
324	300	0.013575	230	300	20	345
325	302.75	0.014628	250	300	20	345
326	300.1768	0.016217	270	300	20	345
327	305.7594	0.016944	290	300	20	345

Table A1 Continued

Sample No.	*d* (mm)	*ρ*	*Vu* (kN)	*av* (mm)	*fc'* (MPa)	*fy* (MPa)
328	316.5107	0.017023	310	300	20	345
329	349.9959	0.014729	330	300	20	345
330	377.3174	0.01349	350	300	20	345
331	231.4331	0.00977	150	200	25	345
332	286.4493	0.007429	170	200	25	345
333	294.0891	0.007965	190	200	25	345
334	279.6538	0.009735	210	200	25	345
335	267.979	0.011611	230	200	25	345
336	251.9507	0.014357	250	200	25	345
337	298.4151	0.011131	270	200	25	345
338	299.6175	0.011994	290	200	25	345
339	287.4985	0.013978	310	200	25	345
340	300	0.013734	330	200	25	345
341	300	0.014606	350	200	25	345
342	220.0018	0.011757	150	220	25	345
343	293.4824	0.007692	170	220	25	345
344	228.4417	0.014143	190	220	25	345
345	267.8573	0.01142	210	220	25	345
346	281.4418	0.011406	230	220	25	345
347	278	0.012817	250	220	25	345
348	297.8544	0.012136	270	220	25	345
349	300	0.012891	290	220	25	345
350	300	0.013862	310	220	25	345
351	300	0.014834	330	220	25	345
352	301.237	0.015794	350	220	25	345
353	287.0895	0.007546	150	240	25	345
354	262.5062	0.010169	170	240	25	345
355	252.0392	0.012442	190	240	25	345
356	248.7248	0.014275	210	240	25	345
357	288.758	0.011652	230	240	25	345
358	295.1265	0.012283	250	240	25	345
359	300	0.012919	270	240	25	345
360	300	0.013891	290	240	25	345
361	299.9967	0.014962	310	240	25	345
362	300.1963	0.016032	330	240	25	345
363	300	0.017206	350	240	25	345
364	262.8508	0.00957	150	260	25	345
365	293.1875	0.008794	170	260	25	345
366	300.5847	0.009429	190	260	25	345
367	299.4648	0.010607	210	260	25	345
368	297.5625	0.011791	230	260	25	345
369	300	0.012747	250	260	25	345
370	300	0.013819	270	260	25	345
371	301.1406	0.014881	290	260	25	345
372	300	0.016162	310	260	25	345
373	300.925	0.017225	330	260	25	345
374	320.006	0.016118	350	260	25	345

Table A1 Continued

Sample No.	*d* (mm)	*ρ*	*Vu* (kN)	*av* (mm)	*fc'* (MPa)	*fy* (MPa)
375	286.6166	0.008548	150	280	25	345
376	281.8717	0.010154	170	280	25	345
377	280.2062	0.011547	190	280	25	345
378	300.308	0.011202	210	280	25	345
379	299.7598	0.012477	230	280	25	345
380	300	0.013547	250	280	25	345
381	299.9922	0.014819	270	280	25	345
382	300.5732	0.015986	290	280	25	345
383	300.0082	0.017262	310	280	25	345
384	302.5529	0.01821	330	280	25	345
385	303.9904	0.019266	350	280	25	345
386	300.2031	0.008387	150	300	25	345
387	300.0417	0.00956	170	300	25	345
388	301.001	0.010626	190	300	25	345
389	300	0.012004	210	300	25	345
390	300	0.013175	230	300	25	345
391	311	0.013471	250	300	25	345
392	300	0.015819	270	300	25	345
393	300.4717	0.017087	290	300	25	345
394	301.2383	0.018251	310	300	25	345
395	300.1791	0.019832	330	300	25	345
396	310.4961	0.019704	350	300	25	345
397	234.7493	0.009446	150	200	30	345
398	281.7476	0.007555	170	200	30	345
399	257.1965	0.010103	190	200	30	345
400	227.4973	0.014278	210	200	30	345
401	300.5706	0.009172	230	200	30	345
402	295.6549	0.010379	250	200	30	345
403	303.6771	0.010691	270	200	30	345
404	296.352	0.012121	290	200	30	345
405	300	0.012662	310	200	30	345
406	299.9965	0.013534	330	200	30	345
407	300.0051	0.014406	350	200	30	345
408	243.759	0.009485	150	220	30	345
409	296.8046	0.007476	170	220	30	345
410	236.3881	0.012971	190	220	30	345
411	268.0981	0.011218	210	220	30	345
412	298.3732	0.010086	230	220	30	345
413	293.9765	0.011291	250	220	30	345
414	299.3957	0.011824	270	220	30	345
415	287.9006	0.013795	290	220	30	345
416	300	0.013662	310	220	30	345
417	300.9189	0.014525	330	220	30	345
418	300.0207	0.015606	350	220	30	345
419	269.4873	0.008434	150	240	30	345
420	248.4294	0.011263	170	240	30	345
421	280.1323	0.010048	190	240	30	345

Table A1 Continued

Sample No.	*d* (mm)	*ρ*	*Vu* (kN)	*av* (mm)	*fc'* (MPa)	*fy* (MPa)
422	298.3531	0.009813	210	240	30	345
423	299.0488	0.010782	230	240	30	345
424	297.1445	0.011968	250	240	30	345
425	300	0.012719	270	240	30	345
426	300	0.013691	290	240	30	345
427	299.9989	0.014762	310	240	30	345
428	300.0015	0.015734	330	240	30	345
429	300.6469	0.016799	350	240	30	345
430	267.8418	0.009143	150	260	30	345
431	293.4257	0.008693	170	260	30	345
432	267.7433	0.011728	190	260	30	345
433	290.7934	0.011061	210	260	30	345
434	298.2295	0.011587	230	260	30	345
435	299.9981	0.012547	250	260	30	345
436	300.0017	0.013619	270	260	30	345
437	300	0.014691	290	260	30	345
438	300.0387	0.015862	310	260	30	345
439	299.5087	0.017039	330	260	30	345
440	299.9863	0.018106	350	260	30	345
441	287.8565	0.008443	150	280	30	345
442	281.0469	0.010058	170	280	30	345
443	301.1976	0.009925	190	280	30	345
444	284.0036	0.012405	210	280	30	345
445	300	0.012275	230	280	30	345
446	300	0.013347	250	280	30	345
447	300	0.014519	270	280	30	345
448	325.1695	0.013398	290	280	30	345
449	300.417	0.016859	310	280	30	345
450	300.3136	0.018031	330	280	30	345
451	301.4671	0.019191	350	280	30	345
452	300.3945	0.008287	150	300	30	345
453	300.0215	0.00946	170	300	30	345
454	300.1953	0.010631	190	300	30	345
455	300.0058	0.011804	210	300	30	345
456	300	0.012975	230	300	30	345
457	300.0049	0.014247	250	300	30	345
458	300	0.015519	270	300	30	345
459	306.8203	0.015935	290	300	30	345
460	300	0.018062	310	300	30	345
461	300	0.019334	330	300	30	345
462	300	0.020606	350	300	30	345
463	237.2833	0.009129	150	200	35	345
464	263.391	0.008563	170	200	35	345
465	229.7881	0.01253	190	200	35	345
466	219.8625	0.015161	210	200	35	345
467	246.936	0.0133	230	200	35	345
468	288.6323	0.010732	250	200	35	345

Table A1 Continued

Sample No.	*d* (mm)	*ρ*	*Vu* (kN)	*av* (mm)	*fc'* (MPa)	*fy* (MPa)
469	289.1885	0.011606	270	200	35	345
470	299.8866	0.011692	290	200	35	345
471	296.538	0.012793	310	200	35	345
472	287.9375	0.014453	330	200	35	345
473	300.0015	0.014306	350	200	35	345
474	220	0.011457	150	220	35	345
475	283.8658	0.008043	170	220	35	345
476	283.4147	0.009027	190	220	35	345
477	233.7544	0.014615	210	220	35	345
478	296.0247	0.010202	230	220	35	345
479	290.9357	0.011414	250	220	35	345
480	299.0898	0.011826	270	220	35	345
481	300	0.012591	290	220	35	345
482	299.7832	0.013564	310	220	35	345
483	300.1432	0.014433	330	220	35	345
484	300.0099	0.015406	350	220	35	345
485	266.8508	0.008548	150	240	35	345
486	263.3696	0.009963	170	240	35	345
487	272.5913	0.010496	190	240	35	345
488	300.0961	0.009703	210	240	35	345
489	295.3289	0.011007	230	240	35	345
490	299.7804	0.011649	250	240	35	345
491	300	0.012619	270	240	35	345
492	300	0.013591	290	240	35	345
493	301.2665	0.014451	310	240	35	345
494	300.25	0.015532	330	240	35	345
495	300.1511	0.016604	350	240	35	345
496	285.8391	0.007952	150	260	35	345
497	266.7446	0.010442	170	260	35	345
498	271.3516	0.011304	190	260	35	345
499	295.9917	0.010628	210	260	35	345
500	298.3748	0.011486	230	260	35	345
501	300	0.012447	250	260	35	345
502	300	0.013519	270	260	35	345
503	300.0054	0.014591	290	260	35	345
504	301.957	0.015445	310	260	35	345
505	299.1719	0.016842	330	260	35	345
506	300.0032	0.017806	350	260	35	345
507	281.4673	0.008773	150	280	35	345
508	283.8732	0.009843	170	280	35	345
509	291.4692	0.01048	190	280	35	345
510	283.0041	0.012312	210	280	35	345
511	300	0.012075	230	280	35	345
512	300.7461	0.013142	250	280	35	345
513	300.0008	0.014419	270	280	35	345
514	298.8125	0.015601	290	280	35	345
515	299.6504	0.016665	310	280	35	345

Table A1 Continued

Sample No.	d (mm)	ρ	Vu (kN)	av (mm)	fc' (MPa)	fy (MPa)
516	299.9942	0.017834	330	280	35	345
517	300.3921	0.019002	350	280	35	345
518	300.2107	0.008187	150	300	35	345
519	309.8483	0.008814	170	300	35	345
520	300	0.010532	190	300	35	345
521	300.0229	0.011703	210	300	35	345
522	300	0.012875	230	300	35	345
523	300	0.014047	250	300	35	345
524	300.2158	0.015217	270	300	35	345
525	300.8711	0.016383	290	300	35	345
526	300.7012	0.017656	310	300	35	345
527	300.1123	0.018933	330	300	35	345
528	300.0336	0.020306	350	300	35	345
529	235.3926	0.007849	150	200	20	420
530	230.1657	0.009463	170	200	20	420
531	293.7594	0.006569	190	200	20	420
532	265.4192	0.008974	210	200	20	420
533	260.3223	0.01027	230	200	20	420
534	264.8928	0.010897	250	200	20	420
535	293.9133	0.009644	270	200	20	420
536	299.298	0.010051	290	200	20	420
537	305.0623	0.010351	310	200	20	420
538	299.2736	0.011534	330	200	20	420
539	300.4451	0.012265	350	200	20	420
540	250.3017	0.007568	150	220	20	420
541	246.8145	0.008958	170	220	20	420
542	280.1585	0.007835	190	220	20	420
543	255.9297	0.010537	210	220	20	420
544	283.9617	0.009414	230	220	20	420
545	273.9487	0.011031	250	220	20	420
546	264.0684	0.013064	270	220	20	420
547	282.2836	0.012274	290	220	20	420
548	288.9986	0.01267	310	220	20	420
549	300	0.012528	330	220	20	420
550	300.0002	0.013469	350	220	20	420
551	246.3601	0.008489	150	240	20	420
552	272.8995	0.007918	170	240	20	420
553	267.1733	0.009305	190	240	20	420
554	252.0298	0.011763	210	240	20	420
555	261	0.012065	230	240	20	420
556	288.9523	0.010731	250	240	20	420
557	297.4688	0.011021	270	240	20	420
558	295.8168	0.012075	290	240	20	420
559	300.0059	0.012687	310	240	20	420
560	300.0293	0.013628	330	240	20	420
561	300.1262	0.014568	350	240	20	420
562	274.3173	0.007357	150	260	20	420

Table A1 Continued

Sample No.	*d* (mm)	*ρ*	*Vu* (kN)	*av* (mm)	*fc'* (MPa)	*fy* (MPa)
563	274.5525	0.00841	170	260	20	420
564	264.4947	0.01022	190	260	20	420
565	267.7144	0.01116	210	260	20	420
566	283.2361	0.011019	230	260	20	420
567	300.3737	0.010661	250	260	20	420
568	293.9878	0.012144	270	260	20	420
569	300	0.012646	290	260	20	420
570	300.8135	0.013581	310	260	20	420
571	301.371	0.014517	330	260	20	420
572	315.1098	0.014151	350	260	20	420
573	280.2179	0.007533	150	280	20	420
574	280.0742	0.008585	170	280	20	420
575	287.3272	0.0092	190	280	20	420
576	283.9876	0.010565	210	280	20	420
577	300.0835	0.010422	230	280	20	420
578	299.898	0.011464	250	280	20	420
579	300.0021	0.012505	270	280	20	420
580	301.4161	0.013436	290	280	20	420
581	301.2092	0.014578	310	280	20	420
582	318.4986	0.013893	330	280	20	420
583	337.2685	0.013096	350	280	20	420
584	302.3545	0.00685	150	300	20	420
585	300	0.007999	170	300	20	420
586	307.3555	0.008608	190	300	20	420
587	300.25	0.01008	210	300	20	420
588	300.0261	0.011122	230	300	20	420
589	300	0.012264	250	300	20	420
590	300.0049	0.013405	270	300	20	420
591	300.6458	0.014441	290	300	20	420
592	315.8995	0.014077	310	300	20	420
593	336.0487	0.013178	330	300	20	420
594	364.1382	0.011934	350	300	20	420
595	234.5483	0.007853	150	200	25	420
596	270.7114	0.006729	170	200	25	420
597	231.8224	0.010335	190	200	25	420
598	281.2121	0.00788	210	200	25	420
599	297.2675	0.007837	230	200	25	420
600	300.5045	0.008361	250	200	25	420
601	234.9772	0.014832	270	200	25	420
602	267.3123	0.012296	290	200	25	420
603	295.108	0.010923	310	200	25	420
604	296.2752	0.011557	330	200	25	420
605	298.379	0.012183	350	200	25	420
606	227.2127	0.009097	150	220	25	420
607	291.8079	0.006333	170	220	25	420
608	255.536	0.009274	190	220	25	420
609	292.9104	0.007917	210	220	25	420

Table A1 Continued

Sample No.	*d* (mm)	*ρ*	*Vu* (kN)	*av* (mm)	*fc'* (MPa)	*fy* (MPa)
610	227.3394	0.014441	230	220	25	420
611	265.8808	0.01149	250	220	25	420
612	297.7737	0.010019	270	220	25	420
613	267.9961	0.01329	290	220	25	420
614	296.4964	0.011713	310	220	25	420
615	296.9768	0.012452	330	220	25	420
616	300.0006	0.013069	350	220	25	420
617	251.4928	0.007962	150	240	25	420
618	276.5642	0.007601	170	240	25	420
619	280.8418	0.008232	190	240	25	420
620	286.4325	0.008852	210	240	25	420
621	299.9456	0.008923	230	240	25	420
622	267.2541	0.01228	250	240	25	420
623	300.0596	0.010604	270	240	25	420
624	298.1941	0.011558	290	240	25	420
625	300	0.012287	310	240	25	420
626	300	0.013228	330	240	25	420
627	299.9961	0.014069	350	240	25	420
628	287.059	0.006606	150	260	25	420
629	263.7563	0.008864	170	260	25	420
630	268.9636	0.009695	190	260	25	420
631	261.4492	0.0114	210	260	25	420
632	293.7764	0.009975	230	260	25	420
633	293.7383	0.010901	250	260	25	420
634	299.6524	0.011407	270	260	25	420
635	300	0.012246	290	260	25	420
636	300	0.013287	310	260	25	420
637	299.5264	0.014232	330	260	25	420
638	299.9922	0.015169	350	260	25	420
639	280.6386	0.007331	150	280	25	420
640	290.5934	0.007838	170	280	25	420
641	297.4602	0.008452	190	280	25	420
642	299.5802	0.009284	210	280	25	420
643	280	0.011738	230	280	25	420
644	297.5752	0.011378	250	280	25	420
645	300	0.012105	270	280	25	420
646	300	0.013146	290	280	25	420
647	311.9233	0.013103	310	280	25	420
648	310.3783	0.01415	330	280	25	420
649	299.1406	0.016376	350	280	25	420
650	300.4531	0.006857	150	300	25	420
651	301.1001	0.007795	170	300	25	420
652	300.0012	0.00884	190	300	25	420
653	300.2148	0.00988	210	300	25	420
654	300.0414	0.010822	230	300	25	420
655	300	0.011864	250	300	25	420
656	300	0.013005	270	300	25	420

Table A1 Continued

Sample No.	*d* (mm)	*ρ*	*Vu* (kN)	*av* (mm)	*fc'* (MPa)	*fy* (MPa)
657	300.9715	0.013939	290	300	25	420
658	300	0.015187	310	300	25	420
659	319.5043	0.014186	330	300	25	420
660	306.4349	0.016617	350	300	25	420
661	239.0977	0.007428	150	200	30	420
662	229	0.009271	170	200	30	420
663	271.4542	0.007481	190	200	30	420
664	264.0067	0.008783	210	200	30	420
665	296.7472	0.00774	230	200	30	420
666	222.9216	0.014873	250	200	30	420
667	250.0033	0.012786	270	200	30	420
668	302.428	0.009529	290	200	30	420
669	280.2874	0.011841	310	200	30	420
670	299.2071	0.011134	330	200	30	420
671	290.6689	0.012548	350	200	30	420
672	220.5391	0.009439	150	220	30	420
673	264.0128	0.007663	170	220	30	420
674	234.1894	0.010817	190	220	30	420
675	251.7656	0.010465	210	220	30	420
676	295.6879	0.008446	230	220	30	420
677	268	0.011174	250	220	30	420
678	267.7182	0.012134	270	220	30	420
679	264.6625	0.013419	290	220	30	420
680	283.4222	0.012615	310	220	30	420
681	292.3947	0.012689	330	220	30	420
682	300	0.012769	350	220	30	420
683	256.1676	0.007639	150	240	30	420
684	269.2501	0.007936	170	240	30	420
685	272.121	0.008678	190	240	30	420
686	275.9893	0.00941	210	240	30	420
687	272.6592	0.010585	230	240	30	420
688	289.9369	0.010325	250	240	30	420
689	268.1316	0.013031	270	240	30	420
690	291.902	0.011903	290	240	30	420
691	295.7525	0.012418	310	240	30	420
692	299.9966	0.012928	330	240	30	420
693	300.0441	0.013769	350	240	30	420
694	281.6066	0.006827	150	260	30	420
695	266.0119	0.008653	170	260	30	420
696	263.1134	0.009928	190	260	30	420
697	260.0583	0.011309	210	260	30	420
698	267.9233	0.011817	230	260	30	420
699	291.4462	0.010915	250	260	30	420
700	306.8889	0.010662	270	260	30	420
701	300	0.012046	290	260	30	420
702	300	0.012987	310	260	30	420
703	301.2485	0.013818	330	260	30	420

Table A1 Continued

Sample No.	d (mm)	ρ	Vu (kN)	av (mm)	fc' (MPa)	fy (MPa)
704	300.0025	0.014869	350	260	30	420
705	280.1326	0.007333	150	280	30	420
706	283.9941	0.008167	170	280	30	420
707	292.4219	0.008675	190	280	30	420
708	287.3681	0.009947	210	280	30	420
709	291.6398	0.010669	230	280	30	420
710	283.348	0.012367	250	280	30	420
711	300	0.011905	270	280	30	420
712	300	0.012946	290	280	30	420
713	300.3018	0.013885	310	280	30	420
714	300.0074	0.014928	330	280	30	420
715	299.9961	0.015869	350	280	30	420
716	300.0011	0.006758	150	300	30	420
717	300.0114	0.007799	170	300	30	420
718	300.0012	0.00874	190	300	30	420
719	311.3096	0.009028	210	300	30	420
720	300.4189	0.01062	230	300	30	420
721	300.0341	0.011663	250	300	30	420
722	300	0.012705	270	300	30	420
723	300.004	0.013746	290	300	30	420
724	300.0025	0.014787	310	300	30	420
725	300.4977	0.015824	330	300	30	420
726	319.9844	0.014815	350	300	30	420
727	203.9424	0.010057	150	200	35	420
728	230.9141	0.009058	170	200	35	420
729	219.9194	0.011128	190	200	35	420
730	250.6272	0.009673	210	200	35	420
731	236.0099	0.011963	230	200	35	420
732	236.131	0.013041	250	200	35	420
733	279.8398	0.010142	270	200	35	420
734	286.0881	0.010545	290	200	35	420
735	250.3438	0.014621	310	200	35	420
736	298.6292	0.011139	330	200	35	420
737	267.9415	0.014565	350	200	35	420
738	229.8291	0.008681	150	220	35	420
739	250.9369	0.008334	170	220	35	420
740	267.6136	0.008303	190	220	35	420
741	231.3215	0.012221	210	220	35	420
742	252.6076	0.011327	230	220	35	420
743	285.0085	0.009756	250	220	35	420
744	276.3689	0.011268	270	220	35	420
745	291.9325	0.010902	290	220	35	420
746	297.7148	0.011304	310	220	35	420
747	291.0077	0.0126	330	220	35	420
748	300	0.012669	350	220	35	420
749	298.8438	0.005662	150	240	35	420
750	282.2377	0.007175	170	240	35	420

Table A1 Continued

Sample No.	*d* (mm)	*ρ*	*Vu* (kN)	*av* (mm)	*fc'* (MPa)	*fy* (MPa)
751	290.8594	0.007583	190	240	35	420
752	256.5381	0.010732	210	240	35	420
753	281.6686	0.009828	230	240	35	420
754	295.5855	0.00979	250	240	35	420
755	298.0583	0.010517	270	240	35	420
756	303.123	0.010925	290	240	35	420
757	300.3641	0.011984	310	240	35	420
758	300	0.012828	330	240	35	420
759	300	0.013669	350	240	35	420
760	274.5827	0.007056	150	260	35	420
761	280.0132	0.007785	170	260	35	420
762	265.762	0.009713	190	260	35	420
763	260.346	0.011207	210	260	35	420
764	278.5516	0.010748	230	260	35	420
765	283.8323	0.011364	250	260	35	420
766	301.321	0.010996	270	260	35	420
767	302.5	0.011729	290	260	35	420
768	300	0.012787	310	260	35	420
769	300	0.013728	330	260	35	420
770	300	0.014669	350	260	35	420
771	280.3199	0.007232	150	280	35	420
772	296.0517	0.007415	170	280	35	420
773	296.8134	0.008355	190	280	35	420
774	291.2383	0.009626	210	280	35	420
775	298.6647	0.01003	230	280	35	420
776	290.8497	0.011519	250	280	35	420
777	300.8659	0.011699	270	280	35	420
778	300	0.012746	290	280	35	420
779	300.0114	0.013687	310	280	35	420
780	301.7471	0.014515	330	280	35	420
781	300.607	0.015564	350	280	35	420
782	300.875	0.006755	150	300	35	420
783	300.2656	0.007698	170	300	35	420
784	300.1553	0.00864	190	300	35	420
785	305.4472	0.009255	210	300	35	420
786	300.8125	0.010518	230	300	35	420
787	300.1094	0.011563	250	300	35	420
788	300	0.012505	270	300	35	420
789	300	0.013546	290	300	35	420
790	300	0.014587	310	300	35	420
791	300.3301	0.015525	330	300	35	420
792	300.0002	0.016669	350	300	35	420
793	235.9825	0.011547	150	200	40	276
794	243.6833	0.012347	170	200	40	276
795	291.7041	0.009898	190	200	40	276
796	276.2822	0.012148	210	200	40	276
797	279.8993	0.013046	230	200	40	276

Table A1 Continued

Sample No.	d (mm)	ρ	Vu (kN)	av (mm)	fc' (MPa)	fy (MPa)
798	302.332	0.012263	250	200	40	276
799	299.709	0.013501	270	200	40	276
800	300.2461	0.014511	290	200	40	276
801	300	0.015628	310	200	40	276
802	300.0029	0.016643	330	200	40	276
803	299.4983	0.017764	350	200	40	276
804	230.6758	0.012994	150	220	40	276
805	251.1837	0.01258	170	220	40	276
806	236.1018	0.015892	190	220	40	276
807	299.3891	0.011259	210	220	40	276
808	301.9712	0.012153	230	220	40	276
809	300.0055	0.013484	250	220	40	276
810	299.516	0.014603	270	220	40	276
811	299.2383	0.015721	290	220	40	276
812	300.4418	0.016823	310	220	40	276
813	298.7813	0.018157	330	220	40	276
814	299.4981	0.019164	350	220	40	276
815	286.9454	0.009284	150	240	40	276
816	299.7366	0.009727	170	240	40	276
817	298.1426	0.010952	190	240	40	276
818	300.4105	0.012051	210	240	40	276
819	299.7773	0.013271	230	240	40	276
820	299.5005	0.014488	250	240	40	276
821	300.0206	0.015598	270	240	40	276
822	302.3837	0.016589	290	240	40	276
823	299.9824	0.018128	310	240	40	276
824	307.7033	0.018354	330	240	40	276
825	299.1432	0.020668	350	240	40	276
826	268.6226	0.011198	150	260	40	276
827	264.1011	0.013173	170	260	40	276
828	289.5014	0.012414	190	260	40	276
829	300	0.012854	210	260	40	276
830	300.2218	0.014067	230	260	40	276
831	300.0009	0.015384	250	260	40	276
832	300	0.016699	270	260	40	276
833	308.9893	0.017023	290	260	40	276
834	315.9508	0.01746	310	260	40	276
835	299.1073	0.020753	330	260	40	276
836	301.4474	0.021839	350	260	40	276
837	284	0.010701	150	280	40	276
838	300.2736	0.010923	170	280	40	276
839	300	0.01234	190	280	40	276
840	299.5052	0.013758	210	280	40	276
841	297.1265	0.015293	230	280	40	276
842	305.3474	0.015837	250	280	40	276
843	299.9901	0.017799	270	280	40	276
844	300.8292	0.019105	290	280	40	276

Table A1 Continued

Sample No.	*d* (mm)	*ρ*	*Vu* (kN)	*av* (mm)	*fc'* (MPa)	*fy* (MPa)
845	300.8354	0.020519	310	280	40	276
846	299.6719	0.022147	330	280	40	276
847	301.0461	0.023344	350	280	40	276
848	300	0.01021	150	300	40	276
849	300.0184	0.011625	170	300	40	276
850	300	0.01304	190	300	40	276
851	300.5977	0.01445	210	300	40	276
852	300.0389	0.015969	230	300	40	276
853	303.6292	0.017052	250	300	40	276
854	300.1344	0.018897	270	300	40	276
855	300.6378	0.020307	290	300	40	276
856	301.6935	0.021709	310	300	40	276
857	300.1345	0.023441	330	300	40	276
858	301.2447	0.024842	350	300	40	276
859	235.1992	0.011554	150	200	45	276
860	215.9883	0.015435	170	200	45	276
861	262.101	0.012035	190	200	45	276
862	232.4392	0.01671	210	200	45	276
863	295.5128	0.011707	230	200	45	276
864	287.9974	0.013396	250	200	45	276
865	299.1989	0.013506	270	200	45	276
866	300.0022	0.014513	290	200	45	276
867	300.9413	0.015418	310	200	45	276
868	300.2733	0.016539	330	200	45	276
869	299.2422	0.017667	350	200	45	276
870	251.9811	0.010917	150	220	45	276
871	275.8396	0.010485	170	220	45	276
872	265.9251	0.012601	190	220	45	276
873	284.7365	0.012375	210	220	45	276
874	299.0407	0.012377	230	220	45	276
875	299.7012	0.013387	250	220	45	276
876	299.6182	0.014502	270	220	45	276
877	300	0.015613	290	220	45	276
878	299	0.016839	310	220	45	276
879	302.7835	0.01751	330	220	45	276
880	319.6695	0.016826	350	220	45	276
881	305.3611	0.008182	150	240	45	276
882	291.9738	0.010175	170	240	45	276
883	296.2666	0.011065	190	240	45	276
884	283.7738	0.013283	210	240	45	276
885	300	0.013169	230	240	45	276
886	299.9529	0.014384	250	240	45	276
887	302.5072	0.015275	270	240	45	276
888	299.5	0.016818	290	240	45	276
889	310.0234	0.01692	310	240	45	276
890	299.2383	0.019252	330	240	45	276
891	299	0.02057	350	240	45	276

Table A1 Continued

Sample No.	*d* (mm)	*ρ*	*Vu* (kN)	*av* (mm)	*fc'* (MPa)	*fy* (MPa)
892	276.9612	0.010544	150	260	45	276
893	283.7422	0.01143	170	260	45	276
894	292.766	0.01209	190	260	45	276
895	300	0.012754	210	260	45	276
896	300	0.014069	230	260	45	276
897	300.0018	0.015384	250	260	45	276
898	305.5376	0.016046	270	260	45	276
899	301.9857	0.017693	290	260	45	276
900	304.5998	0.018678	310	260	45	276
901	303.7545	0.019999	330	260	45	276
902	300.1244	0.021856	350	260	45	276
903	299.8674	0.009611	150	280	45	276
904	289.242	0.011693	170	280	45	276
905	299.9968	0.01224	190	280	45	276
906	300.333	0.013552	210	280	45	276
907	300.4414	0.014966	230	280	45	276
908	300.0068	0.016284	250	280	45	276
909	299.9965	0.017699	270	280	45	276
910	302.1569	0.018791	290	280	45	276
911	300.0139	0.020428	310	280	45	276
912	300.0073	0.021843	330	280	45	276
913	300.0305	0.023257	350	280	45	276
914	306.2988	0.009777	150	300	45	276
915	300.0007	0.011625	170	300	45	276
916	300	0.01304	190	300	45	276
917	300.5898	0.01435	210	300	45	276
918	300.1396	0.015868	230	300	45	276
919	301.1909	0.017173	250	300	45	276
920	301.092	0.018688	270	300	45	276
921	300.0088	0.020213	290	300	45	276
922	300.9805	0.021617	310	300	45	276
923	300.0014	0.023243	330	300	45	276
924	301.0685	0.024544	350	300	45	276
925	211.6183	0.011326	150	200	40	345
926	230.4243	0.011001	170	200	40	345
927	290.5714	0.007985	190	200	40	345
928	259.1465	0.010988	210	200	40	345
929	236.7575	0.014303	230	200	40	345
930	281.8341	0.011185	250	200	40	345
931	298.6726	0.010929	270	200	40	345
932	300.0156	0.01159	290	200	40	345
933	302.8692	0.012237	310	200	40	345
934	299.5742	0.013338	330	200	40	345
935	300.2461	0.014103	350	200	40	345
936	267.5443	0.007845	150	220	40	345
937	289.8302	0.007711	170	220	40	345
938	286.9287	0.008806	190	220	40	345

Table A1 Continued

Sample No.	*d* (mm)	*ρ*	*Vu* (kN)	*av* (mm)	*fc'* (MPa)	*fy* (MPa)
939	270.5135	0.0109	210	220	40	345
940	283.2561	0.010992	230	220	40	345
941	288.2517	0.011635	250	220	40	345
942	296.8992	0.011843	270	220	40	345
943	300	0.012591	290	220	40	345
944	300.167	0.013461	310	220	40	345
945	299.975	0.014334	330	220	40	345
946	300	0.015306	350	220	40	345
947	297.7189	0.006898	150	240	40	345
948	264.3839	0.009857	170	240	40	345
949	264.7874	0.011049	190	240	40	345
950	282.0524	0.010818	210	240	40	345
951	309.9399	0.009912	230	240	40	345
952	291.5712	0.012209	250	240	40	345
953	299.1415	0.012625	270	240	40	345
954	300	0.013491	290	240	40	345
955	300.0002	0.014462	310	240	40	345
956	300.002	0.015434	330	240	40	345
957	302.563	0.01618	350	240	40	345
958	280.4061	0.008278	150	260	40	345
959	266.4142	0.010344	170	260	40	345
960	295.9375	0.009554	190	260	40	345
961	269.8203	0.012605	210	260	40	345
962	282.2188	0.0127	230	260	40	345
963	300.0013	0.012347	250	260	40	345
964	300	0.013419	270	260	40	345
965	301.3255	0.01428	290	260	40	345
966	300.385	0.015459	310	260	40	345
967	300.0072	0.016534	330	260	40	345
968	299.9976	0.017606	350	260	40	345
969	280.329	0.008779	150	280	40	345
970	282.9739	0.009848	170	280	40	345
971	282.3125	0.011134	190	280	40	345
972	283.2108	0.01221	210	280	40	345
973	300	0.012075	230	280	40	345
974	299.9986	0.013147	250	280	40	345
975	300	0.014219	270	280	40	345
976	300	0.015391	290	280	40	345
977	301.7034	0.016347	310	280	40	345
978	303.7461	0.017199	330	280	40	345
979	300.0869	0.018805	350	280	40	345
980	300.3164	0.008187	150	300	40	345
981	300.5625	0.009257	170	300	40	345
982	300.7902	0.010427	190	300	40	345
983	302	0.011492	210	300	40	345
984	300	0.012775	230	300	40	345
985	300	0.013947	250	300	40	345

Table A1 Continued

Sample No.	*d* (mm)	*ρ*	*Vu* (kN)	*av* (mm)	*fc'* (MPa)	*fy* (MPa)
986	300.0002	0.015119	270	300	40	345
987	300.8447	0.016284	290	300	40	345
988	320.5867	0.015391	310	300	40	345
989	300.0417	0.018734	330	300	40	345
990	300.0126	0.020006	350	300	40	345
991	231.3816	0.00957	150	200	45	345
992	249.1865	0.009458	170	200	45	345
993	284.4088	0.008221	190	200	45	345
994	264.6741	0.010444	210	200	45	345
995	251.7672	0.012654	230	200	45	345
996	287.742	0.010739	250	200	45	345
997	291.8435	0.011284	270	200	45	345
998	285.2137	0.01272	290	200	45	345
999	296.7359	0.012692	310	200	45	345
1000	298.455	0.013349	330	200	45	345
1001	300	0.014106	350	200	45	345
1002	276.5986	0.007397	150	220	45	345
987	300.8447	0.016284	290	300	40	345
988	320.5867	0.015391	310	300	40	345
989	300.0417	0.018734	330	300	40	345
990	300.0126	0.020006	350	300	40	345
991	231.3816	0.00957	150	200	45	345
992	249.1865	0.009458	170	200	45	345
993	284.4088	0.008221	190	200	45	345
994	264.6741	0.010444	210	200	45	345
995	251.7672	0.012654	230	200	45	345
996	287.742	0.010739	250	200	45	345
997	291.8435	0.011284	270	200	45	345
998	285.2137	0.01272	290	200	45	345
999	296.7359	0.012692	310	200	45	345
1000	298.455	0.013349	330	200	45	345
1001	300	0.014106	350	200	45	345
1002	276.5986	0.007397	150	220	45	345
987	300.8447	0.016284	290	300	40	345
988	320.5867	0.015391	310	300	40	345
885	300	0.013169	230	240	45	276
886	299.9529	0.014384	250	240	45	276
887	302.5072	0.015275	270	240	45	276
888	299.5	0.016818	290	240	45	276
889	310.0234	0.01692	310	240	45	276
890	299.2383	0.019252	330	240	45	276
891	299	0.02057	350	240	45	276
892	276.9612	0.010544	150	260	45	276
893	283.7422	0.01143	170	260	45	276
894	292.766	0.01209	190	260	45	276
895	300	0.012754	210	260	45	276
896	300	0.014069	230	260	45	276

Table A1 Continued

Sample No.	*d* (mm)	*ρ*	*Vu* (kN)	*av* (mm)	*fc'* (MPa)	*fy* (MPa)
897	300.0018	0.015384	250	260	45	276
898	305.5376	0.016046	270	260	45	276
899	301.9857	0.017693	290	260	45	276
900	304.5998	0.018678	310	260	45	276
901	303.7545	0.019999	330	260	45	276
902	300.1244	0.021856	350	260	45	276
903	299.8674	0.009611	150	280	45	276
904	289.242	0.011693	170	280	45	276
905	299.9968	0.01224	190	280	45	276
906	300.333	0.013552	210	280	45	276
907	300.4414	0.014966	230	280	45	276
908	300.0068	0.016284	250	280	45	276
909	299.9965	0.017699	270	280	45	276
910	302.1569	0.018791	290	280	45	276
911	300.0139	0.020428	310	280	45	276
912	300.0073	0.021843	330	280	45	276
913	300.0305	0.023257	350	280	45	276
914	306.2988	0.009777	150	300	45	276
915	300.0007	0.011625	170	300	45	276
916	300	0.01304	190	300	45	276
917	300.5898	0.01435	210	300	45	276
918	300.1396	0.015868	230	300	45	276
1003	257.3295	0.009602	170	220	45	345
1004	225.1953	0.013874	190	220	45	345
1005	227.7722	0.015075	210	220	45	345
1006	260.1354	0.012878	230	220	45	345
1007	299.6595	0.01075	250	220	45	345
1008	276.9414	0.013512	270	220	45	345
1009	300.0019	0.012491	290	220	45	345
1010	299.9745	0.013363	310	220	45	345
1011	299.9961	0.014334	330	220	45	345
1012	299.8019	0.015208	350	220	45	345
1013	274.57	0.008008	150	240	45	345
1014	249.9996	0.010852	170	240	45	345
1015	299.7391	0.008633	190	240	45	345
1016	283.7111	0.010607	210	240	45	345
1017	290.9496	0.011137	230	240	45	345
1018	301.25	0.011438	250	240	45	345
1019	300	0.012419	270	240	45	345
1020	300	0.013391	290	240	45	345
1021	299.9952	0.014362	310	240	45	345
1022	299.9912	0.015334	330	240	45	345
1023	299.519	0.016411	350	240	45	345
1024	260	0.009486	150	260	45	345
1025	266.2117	0.010345	170	260	45	345
1026	266.3153	0.011538	190	260	45	345
1027	294.3477	0.010638	210	260	45	345

Table A1 Continued

Sample No.	*d* (mm)	*ρ*	*Vu* (kN)	*av* (mm)	*fc'* (MPa)	*fy* (MPa)
1028	298.2999	0.011387	230	260	45	345
1029	300	0.012247	250	260	45	345
1030	300.0004	0.013319	270	260	45	345
1031	300.124	0.01429	290	260	45	345
1032	299.9828	0.015363	310	260	45	345
1033	306.2316	0.015776	330	260	45	345
1034	301.654	0.017289	350	260	45	345
1035	283.4912	0.008563	150	280	45	345
1036	280.5615	0.009961	170	280	45	345
1055	304.9512	0.017988	330	300	45	345
1056	302.7734	0.019478	350	300	45	345
1057	224.4588	0.008314	150	200	40	420
1058	226.7852	0.009286	170	200	40	420
1059	297.7607	0.00625	190	200	40	420
1060	258.222	0.009021	210	200	40	420
1061	230.3125	0.012414	230	200	40	420
1062	218.9472	0.015017	250	200	40	420
1063	236.0935	0.01402	270	200	40	420
1064	258.9796	0.01267	290	200	40	420
1065	267.9658	0.012648	310	200	40	420
1066	312.0408	0.010138	330	200	40	420
1067	283.3852	0.012914	350	200	40	420
1068	239.6631	0.007925	150	220	40	420
1069	260.6005	0.007681	170	220	40	420
1070	234.5503	0.010614	190	220	40	420
1071	295.4922	0.007604	210	220	40	420
1072	220.3438	0.014709	230	220	40	420
1073	236.2639	0.014039	250	220	40	420
1074	294.2439	0.009942	270	220	40	420
1075	264.0063	0.013225	290	220	40	420
1076	293.7717	0.011533	310	220	40	420
1077	293.6559	0.012278	330	220	40	420
1078	300	0.012569	350	220	40	420
1079	244.0723	0.008301	150	240	40	420
1080	240.7001	0.009695	170	240	40	420
1081	267.1501	0.008905	190	240	40	420
1082	243.6347	0.011824	210	240	40	420
1083	293.2578	0.00906	230	240	40	420
1084	292.0488	0.010012	250	240	40	420
1085	273.7865	0.012287	270	240	40	420
1086	289.0231	0.011924	290	240	40	420
1087	299.9765	0.011887	310	240	40	420
1088	300	0.012728	330	240	40	420
1089	300	0.013469	350	240	40	420
1090	295.5721	0.006174	150	260	40	420
1091	260.0371	0.008884	170	260	40	420
1092	268.3232	0.009399	190	260	40	420

Table A1 Continued

Sample No.	*d* (mm)	*ρ*	*Vu* (kN)	*av* (mm)	*fc'* (MPa)	*fy* (MPa)
1093	293.1809	0.008816	210	260	40	420
1094	266.3473	0.011728	230	260	40	420
1095	267.4121	0.012679	250	260	40	420
1096	297.4996	0.011121	270	260	40	420
1097	296.1063	0.012173	290	260	40	420
1098	300	0.012687	310	260	40	420
1099	299.4989	0.013632	330	260	40	420
1100	300	0.014469	350	260	40	420
1101	283.0927	0.007121	150	280	40	420
1102	282.4419	0.008074	170	280	40	420
1103	284.5003	0.009013	190	280	40	420
1104	284.1356	0.009964	210	280	40	420
1105	291.251	0.010471	230	280	40	420
1106	303.9915	0.010541	250	280	40	420
1107	300.4724	0.011702	270	280	40	420
1108	300	0.012646	290	280	40	420
1109	300.0102	0.013587	310	280	40	420
1110	300.0039	0.014528	330	280	40	420
1111	300.0076	0.015469	350	280	40	420
1112	302.5	0.006649	150	300	40	420
1113	301.3438	0.007594	170	300	40	420
1114	300.0082	0.00864	190	300	40	420
1115	300.0159	0.009581	210	300	40	420
1116	300	0.010523	230	300	40	420
1117	300.248	0.011462	250	300	40	420
1118	300	0.012405	270	300	40	420
1119	300	0.013446	290	300	40	420
1120	300.0036	0.014387	310	300	40	420
1121	302.4971	0.015209	330	300	40	420
1122	300.1886	0.016368	350	300	40	420
1123	217.375	0.00886	150	200	45	420
1124	264.3084	0.006961	170	200	45	420
1125	252.5524	0.008492	190	200	45	420
1126	241.5295	0.01024	210	200	45	420
1127	235.9426	0.011763	230	200	45	420
1128	250.307	0.011414	250	200	45	420
1129	243.9807	0.013042	270	200	45	420
1130	225.9117	0.016417	290	200	45	420
1131	235.9415	0.016181	310	200	45	420
1132	281.6886	0.012279	330	200	45	420
1133	284.887	0.0128	350	200	45	420
1134	220	0.009343	150	220	45	420
1135	254.2927	0.008015	170	220	45	420
1136	263.491	0.008426	190	220	45	420
1137	290.963	0.007827	210	220	45	420
1138	301.8889	0.008012	230	220	45	420
1139	282.7661	0.009871	250	220	45	420

Table A1 Continued

Sample No.	*d* (mm)	*ρ*	*Vu* (kN)	*av* (mm)	*fc'* (MPa)	*fy* (MPa)
1140	286.622	0.010394	270	220	45	420
1141	299.5522	0.010249	290	220	45	420
1142	295.0328	0.011324	310	220	45	420
1143	299.2915	0.011834	330	220	45	420
1144	299.5742	0.012473	350	220	45	420
1145	267.1106	0.006888	150	240	45	420
1146	252.7647	0.008723	170	240	45	420
1147	267.6985	0.008802	190	240	45	420
1148	246.633	0.011402	210	240	45	420
1149	267.3986	0.01082	230	240	45	420
1150	297.7694	0.009577	250	240	45	420
1151	278.9395	0.011749	270	240	45	420
1152	299.2471	0.011051	290	240	45	420
1153	302.2157	0.011671	310	240	45	420
1154	300	0.012628	330	240	45	420
1155	293.9688	0.01392	350	240	45	420
1156	298.9329	0.005962	150	260	45	420
1157	261.1563	0.008778	170	260	45	420
1158	267.7374	0.009402	190	260	45	420
1159	310.512	0.007931	210	260	45	420
1160	301.2636	0.009216	230	260	45	420
1161	295.4456	0.010391	250	260	45	420
1162	279.4217	0.012545	270	260	45	420
1163	291.4766	0.012406	290	260	45	420
1164	300.0011	0.012587	310	260	45	420
1165	300.2646	0.013426	330	260	45	420
1166	299.2031	0.014476	350	260	45	420
1167	281.7155	0.007127	150	280	45	420
1168	280.0572	0.008185	170	280	45	420
1169	280.0619	0.009236	190	280	45	420
1170	306.9719	0.008548	210	280	45	420
1171	282.1233	0.011025	230	280	45	420
1172	296.8008	0.010983	250	280	45	420
1173	299.4701	0.011708	270	280	45	420
1174	300	0.012546	290	280	45	420
1175	300	0.013487	310	280	45	420
1176	298.6777	0.014538	330	280	45	420
1177	300	0.015269	350	280	45	420
1178	300	0.006658	150	300	45	420
1179	300	0.007599	170	300	45	420
1180	300.1875	0.00854	190	300	45	420
1181	302.1719	0.009371	210	300	45	420
1182	300.0139	0.010422	230	300	45	420
1183	300.0127	0.011364	250	300	45	420
1184	300.1592	0.012304	270	300	45	420
1185	300	0.013346	290	300	45	420
1186	300.6596	0.014182	310	300	45	420

Table A1 Continued

Sample No.	*d* (mm)	*ρ*	*Vu* (kN)	*av* (mm)	*fc'* (MPa)	*fy* (MPa)
1187	300	0.015328	330	300	45	420
1188	300.0052	0.016269	350	300	45	420
1189	281.2007	0.004648	150	200	20	500
1190	263.632	0.006046	170	200	20	500
1191	222.1049	0.009721	190	200	20	500
1192	232.1484	0.009908	210	200	20	500
1193	275.4646	0.007684	230	200	20	500
1194	235.4214	0.011788	250	200	20	500
1195	270.6922	0.009573	270	200	20	500
1196	297.5233	0.008533	290	200	20	500
1197	304.6376	0.008709	310	200	20	500
1198	298.8313	0.009763	330	200	20	500
1199	296.8162	0.010596	350	200	20	500
1200	234.9032	0.007235	150	220	20	500
1201	230.9924	0.008608	170	220	20	500
1202	269.0562	0.007155	190	220	20	500
1203	225.0482	0.011559	210	220	20	500
1204	299.1318	0.007067	230	220	20	500
1205	257.5	0.010626	250	220	20	500
1206	255.1953	0.011781	270	220	20	500
1207	293.3435	0.009558	290	220	20	500
1208	276.123	0.011696	310	220	20	500
1209	289.1052	0.011429	330	220	20	500
1210	297.5226	0.011491	350	220	20	500
1211	260.6861	0.006323	150	240	20	500
1212	307.475	0.005283	170	240	20	500
1213	296.7328	0.006338	190	240	20	500
1214	290.4682	0.007385	210	240	20	500
1215	276.8533	0.008977	230	240	20	500
1216	291.4641	0.008825	250	240	20	500
1217	295.3138	0.009425	270	240	20	500
1218	276.3232	0.011766	290	240	20	500
1219	300.2523	0.010635	310	240	20	500
1220	298.2138	0.011567	330	240	20	500
1221	300	0.012274	350	240	20	500
1222	273.4778	0.006175	150	260	20	500
1223	282.0194	0.006672	170	260	20	500
1224	271.9619	0.008142	190	260	20	500
1225	264.8357	0.00961	210	260	20	500
1226	278.2957	0.009569	230	260	20	500
1227	295.6628	0.009203	250	260	20	500
1228	284.7005	0.010986	270	260	20	500
1229	294.0689	0.011053	290	260	20	500
1230	292.389	0.012185	310	260	20	500
1231	300	0.012356	330	260	20	500
1232	309.2028	0.012412	350	260	20	500
1233	281.043	0.006249	150	280	20	500

Table A1 Continued

Sample No.	*d* (mm)	*ρ*	*Vu* (kN)	*av* (mm)	*fc'* (MPa)	*fy* (MPa)
1234	280.0898	0.007279	170	280	20	500
1235	280.1799	0.008206	190	280	20	500
1236	301.0693	0.00784	210	280	20	500
1237	300.3281	0.008761	230	280	20	500
1238	287.8873	0.010544	250	280	20	500
1239	301.8185	0.01039	270	280	20	500
1240	305.8906	0.010985	290	280	20	500
1241	300.0058	0.012337	310	280	20	500
1242	328.8427	0.010884	330	280	20	500
1243	320.0017	0.012344	350	280	20	500
1244	300.025	0.005889	150	300	20	500
1245	300	0.006707	170	300	20	500
1246	300.25	0.007525	190	300	20	500
1247	300.2578	0.008443	210	300	20	500
1248	300.0021	0.009363	230	300	20	500
1249	300.1383	0.010281	250	300	20	500
1250	300.4375	0.011198	270	300	20	500
1251	300	0.012219	290	300	20	500
1252	315.5091	0.011847	310	300	20	500
1253	319.6575	0.012335	330	300	20	500
1254	331.8163	0.012175	350	300	20	500
1255	242.3426	0.0062	150	200	25	500
1256	256.6062	0.006278	170	200	25	500
1257	232.1677	0.008655	190	200	25	500
1258	253.6944	0.008072	210	200	25	500
1259	229.3581	0.010883	230	200	25	500
1260	240.3072	0.010849	250	200	25	500
1261	234.2535	0.012549	270	200	25	500
1262	300.8448	0.008214	290	200	25	500
1263	243.8104	0.01346	310	200	25	500
1264	292.2073	0.010008	330	200	25	500
1265	299.7268	0.010076	350	200	25	500
1266	239.5	0.006813	150	220	25	500
1267	279.2589	0.005782	170	220	25	500
1268	226.0316	0.009894	190	220	25	500
1269	234.4846	0.010292	210	220	25	500
1270	273.4775	0.008295	230	220	25	500
1271	246.7527	0.011201	250	220	25	500
1272	232.0183	0.013969	270	220	25	500
1273	289.8052	0.009579	290	220	25	500
1274	291.25	0.010192	310	220	25	500
1275	271.9365	0.012557	330	220	25	500
1276	299.71	0.010976	350	220	25	500
1277	262.656	0.006115	150	240	25	500
1278	264.1179	0.006944	170	240	25	500
1279	247.762	0.008963	190	240	25	500
1280	284.2588	0.007513	210	240	25	500

Table A1 Continued

Sample No.	*d* (mm)	ρ	*Vu* (kN)	*av* (mm)	*fc'* (MPa)	*fy* (MPa)
1281	267.3425	0.009429	230	240	25	500
1282	261.8917	0.010797	250	240	25	500
1283	295.8716	0.009122	270	240	25	500
1284	305.6178	0.009287	290	240	25	500
1285	283.0905	0.011647	310	240	25	500
1286	296.2627	0.01138	330	240	25	500
1287	298.9354	0.011881	350	240	25	500
1288	260	0.006726	150	260	25	500
1289	260.045	0.007662	170	260	25	500
1290	267.6464	0.008162	190	260	25	500
1291	299.5659	0.007246	210	260	25	500
1292	260.0662	0.010672	230	260	25	500
1293	277.3007	0.010303	250	260	25	500
1294	294.1924	0.009932	270	260	25	500
1295	296	0.010642	290	260	25	500
1296	296.6895	0.011358	310	260	25	500
1297	299.8829	0.011956	330	260	25	500
1298	299.9981	0.012774	350	260	25	500
1299	283.9295	0.006039	150	280	25	500
1300	281.0996	0.007075	170	280	25	500
1301	281.4604	0.0079	190	280	25	500
1302	284.6344	0.008612	210	280	25	500
1303	287.21	0.009324	230	280	25	500
1304	297.8986	0.009492	250	280	25	500
1305	283.9507	0.01149	270	280	25	500
1306	282.0983	0.012628	290	280	25	500
1307	300	0.011937	310	280	25	500
1308	300	0.012756	330	280	25	500
1309	299.9939	0.013674	350	280	25	500
1310	300.0018	0.005789	150	300	25	500
1311	301.4453	0.006503	170	300	25	500
1312	300.0232	0.007426	190	300	25	500
1313	300.0027	0.008244	210	300	25	500
1314	309.25	0.008622	230	300	25	500
1315	300.0202	0.009981	250	300	25	500
1316	301.6506	0.010791	270	300	25	500
1317	300	0.011819	290	300	25	500
1318	300	0.012737	310	300	25	500
1319	300.0092	0.013655	330	300	25	500
1320	300	0.014674	350	300	25	500
1321	200.5195	0.00883	150	200	30	500
1322	240.2288	0.007058	170	200	30	500
1323	214.4688	0.009975	190	200	30	500
1324	269.8604	0.007083	210	200	30	500
1325	231.5581	0.010566	230	200	30	500
1326	232.7314	0.01141	250	200	30	500
1327	283.0379	0.008396	270	200	30	500

Table A1 Continued

Sample No.	*d* (mm)	*ρ*	*Vu* (kN)	*av* (mm)	*fc'* (MPa)	*fy* (MPa)
1328	231.0028	0.013632	290	200	30	500
1329	298.4567	0.008847	310	200	30	500
1330	267.6226	0.011692	330	200	30	500
1331	301.4036	0.009864	350	200	30	500
1332	225.1277	0.007685	150	220	30	500
1333	223.9121	0.00885	170	220	30	500
1334	234.341	0.009041	190	220	30	500
1335	228.7735	0.010632	210	220	30	500
1336	283.2019	0.007644	230	220	30	500
1337	298.5863	0.007588	250	220	30	500
1338	238.8497	0.01281	270	220	30	500
1339	273.9906	0.010482	290	220	30	500
1340	240.875	0.014688	310	220	30	500
1341	283.7783	0.011267	330	220	30	500
1342	298.5881	0.010884	350	220	30	500
1343	246.9811	0.00688	150	240	30	500
1344	241.733	0.00815	170	240	30	500
1345	242.2374	0.009194	190	240	30	500
1346	267.9247	0.008393	210	240	30	500
1347	274.6241	0.008789	230	240	30	500
1348	264.6395	0.010379	250	240	30	500
1349	240.6274	0.013695	270	240	30	500
1350	256.7178	0.013008	290	240	30	500
1351	280.0887	0.011668	310	240	30	500
1352	300.0647	0.010855	330	240	30	500
1353	302.9246	0.011354	350	240	30	500
1354	265.1311	0.006406	150	260	30	500
1355	263.1996	0.007448	170	260	30	500
1356	277.4202	0.007518	190	260	30	500
1357	267.5997	0.008995	210	260	30	500
1358	267.623	0.009928	230	260	30	500
1359	286.6157	0.009451	250	260	30	500
1360	283.8092	0.010491	270	260	30	500
1361	262.4596	0.013364	290	260	30	500
1362	310.5435	0.010175	310	260	30	500
1363	297.3125	0.011873	330	260	30	500
1364	300	0.012474	350	260	30	500
1365	286.1765	0.005932	150	280	30	500
1366	288.6923	0.006647	170	280	30	500
1367	279.9997	0.007906	190	280	30	500
1368	282.0507	0.008624	210	280	30	500
1369	280.9368	0.009655	230	280	30	500
1370	282.1074	0.010475	250	280	30	500
1371	295.4692	0.010325	270	280	30	500
1372	280.6444	0.012437	290	280	30	500
1373	296.9019	0.011956	310	280	30	500
1374	300	0.012456	330	280	30	500

Table A1 Continued

Sample No.	*d* (mm)	*ρ*	*Vu* (kN)	*av* (mm)	*fc'* (MPa)	*fy* (MPa)
1375	300.3574	0.013272	350	280	30	500
1376	300	0.005689	150	300	30	500
1377	300.0618	0.006507	170	300	30	500
1378	300.375	0.007325	190	300	30	500
1379	300.2852	0.008143	210	300	30	500
1380	301.5625	0.008856	230	300	30	500
1381	300.208	0.00988	250	300	30	500
1382	300.0606	0.0107	270	300	30	500
1383	300.1757	0.011518	290	300	30	500
1384	300	0.012437	310	300	30	500
1385	300.625	0.013251	330	300	30	500
1386	300.0045	0.014274	350	300	30	500
1387	208.8665	0.008077	150	200	35	500
1388	212.1446	0.008925	170	200	35	500
1389	236.055	0.008131	190	200	35	500
1390	219.9531	0.010397	210	200	35	500
1391	300.374	0.006361	230	200	35	500
1392	246.2219	0.010105	250	200	35	500
1393	235.9428	0.011934	270	200	35	500
1394	240.9452	0.01234	290	200	35	500
1395	281.8255	0.009756	310	200	35	500
1396	283.3768	0.01027	330	200	35	500
1397	298.8984	0.009882	350	200	35	500
1398	220.0021	0.007912	150	220	35	500
1399	220.002	0.009074	170	220	35	500
1400	234.8542	0.008938	190	220	35	500
1401	296.9389	0.006357	210	220	35	500
1402	233.9635	0.011048	230	220	35	500
1403	248.0352	0.010792	250	220	35	500
1404	235.9375	0.012934	270	220	35	500
1405	301.7623	0.008608	290	220	35	500
1406	233.7513	0.015358	310	220	35	500
1407	299.6571	0.010058	330	220	35	500
1408	298.4159	0.010785	350	220	35	500
1409	282.7881	0.005243	150	240	35	500
1410	254.2954	0.007388	170	240	35	500
1411	305.6335	0.005805	190	240	35	500
1412	281.4971	0.007526	210	240	35	500
1413	297.9231	0.007472	230	240	35	500
1414	295.8235	0.008202	250	240	35	500
1415	275.6685	0.010241	270	240	35	500
1416	267.3453	0.011728	290	240	35	500
1417	266.7344	0.012666	310	240	35	500
1418	299.465	0.0101759	330	240	35	500
1419	299.8175	0.011475	350	240	35	500
1420	260.0738	0.006625	150	260	35	500
1421	260.0264	0.007562	170	260	35	500

Table A1 Continued

Sample No.	*d* (mm)	*ρ*	*Vu* (kN)	*av* (mm)	*fc'* (MPa)	*fy* (MPa)
1422	262.9688	0.008284	190	260	35	500
1423	260.2842	0.009434	210	260	35	500
1424	264	0.010049	230	260	35	500
1425	261.2731	0.011301	250	260	35	500
1426	303.7976	0.00908	270	260	35	500
1427	287.5225	0.010893	290	260	35	500
1428	294.4539	0.011172	310	260	35	500
1429	296	0.011882	330	260	35	500
1430	300	0.012274	350	260	35	500
1431	280.0771	0.006152	150	280	35	500
1432	297.6835	0.006215	170	280	35	500
1433	282.5676	0.007695	190	280	35	500
1434	280.0923	0.008733	210	280	35	500
1435	303.2068	0.008149	230	280	35	500
1436	310.5062	0.008531	250	280	35	500
1437	289.4829	0.010658	270	280	35	500
1438	312.1974	0.009851	290	280	35	500
1439	305.7423	0.011103	310	280	35	500
1440	300	0.012356	330	280	35	500
1441	300	0.013174	350	280	35	500
1442	300.0015	0.005689	150	300	35	500
1443	300.0061	0.006507	170	300	35	500
1444	300.0037	0.007226	190	300	35	500
1445	300.07	0.008044	210	300	35	500
1446	300.0519	0.008863	230	300	35	500
1447	300.0312	0.009681	250	300	35	500
1448	300	0.0105	270	300	35	500
1449	300.4638	0.011316	290	300	35	500
1450	300	0.012237	310	300	35	500
1451	300	0.013156	330	300	35	500
1452	300.0093	0.013974	350	300	35	500
1453	209.9352	0.00797	150	200	40	500
1454	203.7473	0.009583	170	200	40	500
1455	294.8385	0.005346	190	200	40	500
1456	227.8057	0.009639	210	200	40	500
1457	264.287	0.008047	230	200	40	500
1458	222.0058	0.012202	250	200	40	500
1459	261.9148	0.009633	270	200	40	500
1460	267.8489	0.009925	290	200	40	500
1461	268.5165	0.010652	310	200	40	500
1462	265.4909	0.01161	330	200	40	500
1463	248.231	0.014107	350	200	40	500
1464	226.8805	0.007375	150	220	40	500
1465	233.1729	0.007996	170	220	40	500
1466	255.4766	0.007522	190	220	40	500
1467	232.3972	0.010106	210	220	40	500
1468	263.0071	0.008655	230	220	40	500

Table A1 Continued

Sample No.	*d* (mm)	*ρ*	*Vu* (kN)	*av* (mm)	*fc'* (MPa)	*fy* (MPa)
1469	279.0512	0.008493	250	220	40	500
1470	246.1259	0.01175	270	220	40	500
1471	294.9909	0.008948	290	220	40	500
1472	260.0874	0.012219	310	220	40	500
1473	283.8694	0.011067	330	220	40	500
1474	284.644	0.011686	350	220	40	500
1475	240.2104	0.00711	150	240	40	500
1476	304.9087	0.005191	170	240	40	500
1477	260.6434	0.007796	190	240	40	500
1478	283.0924	0.007419	210	240	40	500
1479	285.6889	0.008031	230	240	40	500
1480	265.3567	0.010075	250	240	40	500
1481	279.5563	0.009917	270	240	40	500
1482	280.8831	0.010535	290	240	40	500
1483	291.2087	0.010592	310	240	40	500
1484	289.1241	0.011429	330	240	40	500
1485	294.899	0.01171	350	240	40	500
1486	290.593	0.005318	150	260	40	500
1487	262.1605	0.007353	170	260	40	500
1488	293.0303	0.006653	190	260	40	500
1489	284.6377	0.007812	210	260	40	500
1490	260.1938	0.010271	230	260	40	500
1491	307.1888	0.008147	250	260	40	500
1492	277.7508	0.010728	270	260	40	500
1493	277.5103	0.011558	290	260	40	500
1494	292.0046	0.011287	310	260	40	500
1495	299.558	0.011458	330	260	40	500
1496	300	0.012174	350	260	40	500
1497	280.0219	0.006052	150	280	40	500
1498	299.2638	0.00611	170	280	40	500
1499	281.4877	0.0077	190	280	40	500
1500	290.8149	0.007984	210	280	40	500
1501	295.2987	0.008585	230	280	40	500
1502	286.8239	0.00985	250	280	40	500
1503	282.7164	0.011098	270	280	40	500
1504	299.4656	0.010622	290	280	40	500
1505	310.9812	0.010572	310	280	40	500
1506	300	0.012156	330	280	40	500
1507	300	0.012974	350	280	40	500
1508	301.25	0.005585	150	300	40	500
1509	300	0.006407	170	300	40	500
1510	300	0.007226	190	300	40	500
1511	300.0251	0.008044	210	300	40	500
1512	300.7803	0.008759	230	300	40	500
1513	300.0857	0.009581	250	300	40	500
1514	301.75	0.010291	270	300	40	500
1515	301.0469	0.011213	290	300	40	500

Table A1 Continued

Sample No.	*d* (mm)	*ρ*	*Vu* (kN)	*av* (mm)	*fc'* (MPa)	*fy* (MPa)
1516	300	0.012137	310	300	40	500
1517	300.1592	0.012955	330	300	40	500
1518	300	0.013774	350	300	40	500
1519	210.7919	0.007865	150	200	45	500
1520	227.4064	0.007729	170	200	45	500
1521	215.4002	0.009668	190	200	45	500
1522	221.75	0.010084	210	200	45	500
1523	205.7028	0.012888	230	200	45	500
1524	234.5944	0.010895	250	200	45	500
1525	267.0518	0.009197	270	200	45	500
1526	215.9892	0.015087	290	200	45	500
1527	248.0937	0.012321	310	200	45	500
1528	248.4663	0.013061	330	200	45	500
1529	293.8755	0.010117	350	200	45	500
1530	250.5459	0.006164	150	220	45	500
1531	281.1406	0.005575	170	220	45	500
1532	249.3867	0.007854	190	220	45	500
1533	279.7721	0.007034	210	220	45	500
1534	282.7294	0.007546	230	220	45	500
1535	235.9061	0.011684	250	220	45	500
1536	260	0.010546	270	220	45	500
1537	282.5507	0.009625	290	220	45	500
1538	267.9604	0.011457	310	220	45	500
1539	235.762	0.015788	330	220	45	500
1540	267.4767	0.013126	350	220	45	500
1541	250.1094	0.006566	150	240	45	500
1542	256.9903	0.007176	170	240	45	500
1543	252.9209	0.008236	190	240	45	500
1544	275.4364	0.007755	210	240	45	500
1545	250.2584	0.010334	230	240	45	500
1546	279.7021	0.009089	250	240	45	500
1547	293.8225	0.008934	270	240	45	500
1548	289.2064	0.009883	290	240	45	500
1549	290.3609	0.010598	310	240	45	500
1550	290.7373	0.011218	330	240	45	500
1551	279.2472	0.012928	350	240	45	500
1552	260.2908	0.006524	150	260	45	500
1553	264.3672	0.007243	170	260	45	500
1554	265.1558	0.008074	190	260	45	500
1555	290.1636	0.007487	210	260	45	500
1556	260	0.010273	230	260	45	500
1557	296.3722	0.0087	250	260	45	500
1558	290.9926	0.00975	270	260	45	500
1559	290.0352	0.010578	290	260	45	500
1560	261.1563	0.01391	310	260	45	500
1561	282	0.01278	330	260	45	500
1562	299.7489	0.012076	350	260	45	500

Table A1 Continued

Sample No.	*d* (mm)	*ρ*	*Vu* (kN)	*av* (mm)	*fc'* (MPa)	*fy* (MPa)
1563	280.0008	0.006052	150	280	45	500
1564	280	0.006879	170	280	45	500
1565	284.1237	0.007489	190	280	45	500
1566	280	0.008533	210	280	45	500
1567	282.3825	0.009248	230	280	45	500
1568	291.9741	0.009522	250	280	45	500
1569	284.125	0.010889	270	280	45	500
1570	296.796	0.010737	290	280	45	500
1571	292.5696	0.011884	310	280	45	500
1572	300	0.012056	330	280	45	500
1573	300	0.012874	350	280	45	500
1574	313.5313	0.005151	150	300	45	500
1575	300.25	0.006407	170	300	45	500
1576	372	0.004808	190	300	45	500
1577	301.9219	0.007837	210	300	45	500
1578	300	0.008763	230	300	45	500
1579	300.0028	0.009581	250	300	45	500
1580	300.0202	0.0104	270	300	45	500
1581	300.1924	0.011217	290	300	45	500
1582	300	0.012037	310	300	45	500
1583	300	0.012856	330	300	45	500
1584	300.0045	0.013674	350	300	45	500